Article

Not peer-reviewed version

Synthesis of Temporin-SHa Retro Analogs with Lysine Addition / Substitution and Antibiotic Conjugation to Enhance Antibacterial, Antifungal, and Anticancer Activities

Shahzad Nazir , Arif Iftikhar Khan * , Rukesh Maharjan * , Sadiq Noor Khan , Muhammad Adnan Akram , Marc Maresca * , Farooq-Ahmad Khan , Farzana Shaheen *

Posted Date: 7 November 2024

doi: 10.20944/preprints202411.0510.v1

Keywords: Temporin SHa; levofloxacin; antimicrobial peptides; AMPs; antibacterial; antifungal; anticancer

 doi:10.20944/preprints202411.0510.v1

Article

Synthesis of Temporin-SHa Retro Analogs with Lysine Addition / Substitution and Antibiotic Conjugation to Enhance Antibacterial, Antifungal, and Anticancer Activities

Shahzad Nazir [1], Arif Iftikhar Khan [1], Rukesh Maharjan [1], Sadiq Noor Khan [1], Muhammad Adnan Akram [1], Marc Maresca [2,*], Farooq-Ahmad Khan [1] and Farzana Shaheen [1,*]

[1] Third World Center for Science and Technology, International Center for Chemical and Biological Sciences, University of Karachi, Karachi 75270, Pakistan
[2] Aix Marseille Univ, CNRS, Centrale Med, ISM2, 13013, Marseille, France
* Correspondence: m.maresca@univ-amu.fr (M.M.); afnan.iccs@gmail.com (F.S.); Tel.: +33-0413945609 (M.M.); +92-21111222292 (F.S.)

Abstract: In the face of rising threat of resistant pathogens, antimicrobial peptides (AMPs) offer a viable alternative to the current challenge due to their broad-spectrum activity. This study focuses on enhancing the efficacy of temporin-SHa derived NST-2 peptide (**1**), which is known for its antimicrobial and anticancer activities. We synthesized new analogs of **1** using three strategies, i.e., retro analog preparation, lysine addition/substitution, and levofloxacin conjugation. Analogs were tested in term of antibacterial, antifungal, and anticancer activities. Analog **2** corresponding to retro analog of NST-2 was found more active but also more hemolytic, reducing its selectivity index and therapeutic potential. Addition of lysine (in analog **3**) and lysine substitution (in analog **7**) reduced the hemolytic effect resulting in safer peptides. Conjugation with levofloxacin on lysine side chain (in analogs **4** and **5**) decreased the hemolytic effect but unfortunately also the antimicrobial and anticancer activities of the analogs. Oppositely, conjugation with levofloxacin at the N-terminus of the peptide via β-alanine linker (in analogs **6** and **8**) increased their antimicrobial and anticancer activity but also their hemolytic effect, resulting in less safe/selective analogs. In conclusion, lysine addition/substitution and levofloxacin conjugation, at least at the N-terminal position through β-alanine linker, were found to enhance the therapeutic potential of retro analogs of NST-2 whereas other modifications decreased the activity or increased the toxicity of the peptides.

Keywords: Temporin SHa; levofloxacin; antimicrobial peptides; AMPs; antibacterial; antifungal; anticancer

1. Introduction

The rise of resistant pathogens has drawn attention to antimicrobial peptides (AMPs), which possess broad-spectrum efficacy. AMPs operate through unique mechanism of action that makes it harder for pathogens to develop resistance [1]. Despite this potential, many challenges like instability, protease susceptibility, hemolysis, and toxicity have limited their clinical use. Researchers have explored several ingenious strategies to address these issues. For example, one early method involved swapping the natural L-amino acids with unnatural D-amino acids to makes these peptides invisible to proteases, which typically recognize and cleave natural amino acid chains. This seemingly minor tweak enhances the stability of AMPs in the bloodstream [2]. Another effective approach that has shown promise is peptide cyclization, which not only lowers the toxicity but also improves antimicrobial activity [3]. Researchers have also tried attaching polyethylene glycol (PEG) to peptides (PEGylation), wherein PEG acts as a hydrophilic shield to improve peptide solubility in aqueous

 doi:10.20944/preprints202411.0510.v1

environment. PEGylation was found to enhance the renal clearance of peptides, thereby preventing the unwanted build-up to lower the potential side effects of AMPs [4,5]. Other modifications like glycosylation (attaching sugar molecules) or lipidation (conjugating fatty acids) have extended the functional activities of AMPs [6,7]. Additionally, flipping the order of amino acids to make retro analogs, and reversing the handedness of amino acids to create inverso-analogs, has shown to enhance the potency of AMPs [8]. Taking these two concepts a step further, retro-inverso peptides were also developed, which are basically mirror images of the original molecule with reversed amino acid sequence. This double twist alters the stereochemical and conformational properties of the peptides, potentially leading to new AMPs with beneficial properties [9,10]. All these innovative strategies by researchers offer a glimpse of hope in improving the activities of AMPs, which can pave the way to develop effective antimicrobial therapies. [11].

Conjugating heterocycles with small peptides is also known to improve the biological properties. Since year 2000, numerous heterocyclic-conjugated peptides with potential therapeutic benefits have been reported [12–16]. Likewise, arene-peptide conjugates were also developed with promising medicinal properties [17–20]. Antibiotic drugs like levofloxacin gained our attention due to broad-spectrum antimicrobial effect. Recently, its conjugation with antimicrobial peptide named indolicidin was reported by Ghaffar et al. [21]. Levofloxacin-M33 peptide conjugate did not show any major change in its ability to fight Gram-negative bacteria [22]. Interestingly, when a linear peptide (R4W4) was conjugated with levofloxacin, an improvement of antibacterial activity with low hemolytic effect was observed. [23,24]. Early research looked into retro-analogs of P53 peptides using molecular dynamics simulations and circular dichroism spectroscopy [25,26]. Temporin-SHa is a natural AMP isolated from frog skin. Recently, we used the Fmoc peptide synthesis strategy to prepare its analogs, wherein natural glycine-10 residue of the parent temporin-SHa molecule was replaced with atypical (2-naphthyl)-D-alanine, D-tyrosine and D-phenylalanine to study the effects of hydrophobic residues on antimicrobial efficacy [27]. Previously, we also synthesized [G4a]-SHa, [G7a]-SHa, and [G10a]-SHa analogs by substituting glycine residue with D-alanine at position 4, 7, and 10, respectively [28]. Among these analogs, NST-2, corresponding to [G4a]-SHa peptide, demonstrated promising activity against methicillin-resistant *Staphylococcus aureus* (NCTC 13277) with an MIC of 14.3 μM. It also showed low hemolysis as compared to parent temporin-SHa peptide [29]. These results make this analog a suitable choice for further investigation [30].

The peptide analog NST-2 is D-alanine modified variant of temporin-SHa [28]. In this work, we decided to synthesize NST-2 in a retro manner potentially increasing its activity [31]. Then, we further modified retro analog of NST-2 by either adding lysine residue to its C terminus or by substitution of glycine at the 4th position of this retro analog with lysine. Finally, to potentially further enhance the therapeutic potential of the peptide, we conjugated the antibiotic levofloxacin to either the side chain of lysine-3 or lysine-14 of the retro analog or to the N-terminal phenylalanine-1 via a β-alanine linker. A summary of these modifications in retro analog of NST-2 is provided in Scheme 1.

2. Materials and Methods

2.1. Reagents and Instruments

The reagents used in our experiments were 95–98% pure. Novabiochem (Hohenbrunn, Germany) and Chem-impex (Wood Dale, IL, USA) provided the Fmoc-protected amino acids, Rink amide resin, and coupling reagents. Fmoc protected Rink amide resin had a loading capacity of 0.602 mmol/g and mesh size of 200–300. HPLC grade solvents were employed. All peptides were purified with preparative HPLC (PuriFlash®) by using PFB15C18XS-250/212 column. Purity of peptides was checked via UPLC (Agilent 1260 Infinity Diode Array, C-4 reverse-phase analytical column, 5 μm, and 150 x 4.6 mm). Electrospray ionization mass spectrometer (Q-STAR XL, Applied Biosystems, USA) with quadrupole time-of-flight analyzer (ESI-QTOF-MS) was used for molecular mass determination. NMR spectrometer of 600 MHz (Bruker, Switzerland) was used to record 1D and 2D NMR spectra. Carbon spectra were obtained by adjusting the frequency at 125 MHz.

2.2. Peptides Synthesis and Characterization

Preprints.org (www.preprints.org) | NOT PEER-REVIEWED | Posted: 7 November 2024 doi:10.20944/preprints202411.0510.v1

2.2.1. Synthesis of Temporin-SHa Retro-Analogs and Their Levofloxacin Conjugates

Peptides analogs and their levofloxacin conjugates were manually synthesized by using Fmoc solid phase method on Rink amide resin as shown in Scheme 1. The resin (1 g, 0.6 mmol/g) was soaked in DMF for 2 hours, followed by its treatment with 4-methylpiperidine (20%) to remove the protecting group. Fmoc-Phe-OH (6 equiv.) was then loaded on the resin with the help of 6 equivalents of *N,N'*-diisopropylcarbodiimide (DIC) and 2-cyano-2-(hydroxyimino) acetate (Oxyma pure) as additive to suppress racemization. After the reaction, 4-methylpiperidine in DMF (20%) was added to remove the protecting group and the next amino acid was coupled. Overall, the successive coupling was done by employing 3 equivalents each of Fmoc-protected amino acids, coupling reagent and additive. Levofloxacin was coupled with peptide sequences at different position after the removal of Alloc and Fmoc protecting groups. The peptides were then cleaved from the resin with TFA cocktail (94% TFA, 1% triisopropylsilane, 2.5% ethanedithiol, 2.5% water). The crude peptide was precipitated with diethyl ether and lyophilized.

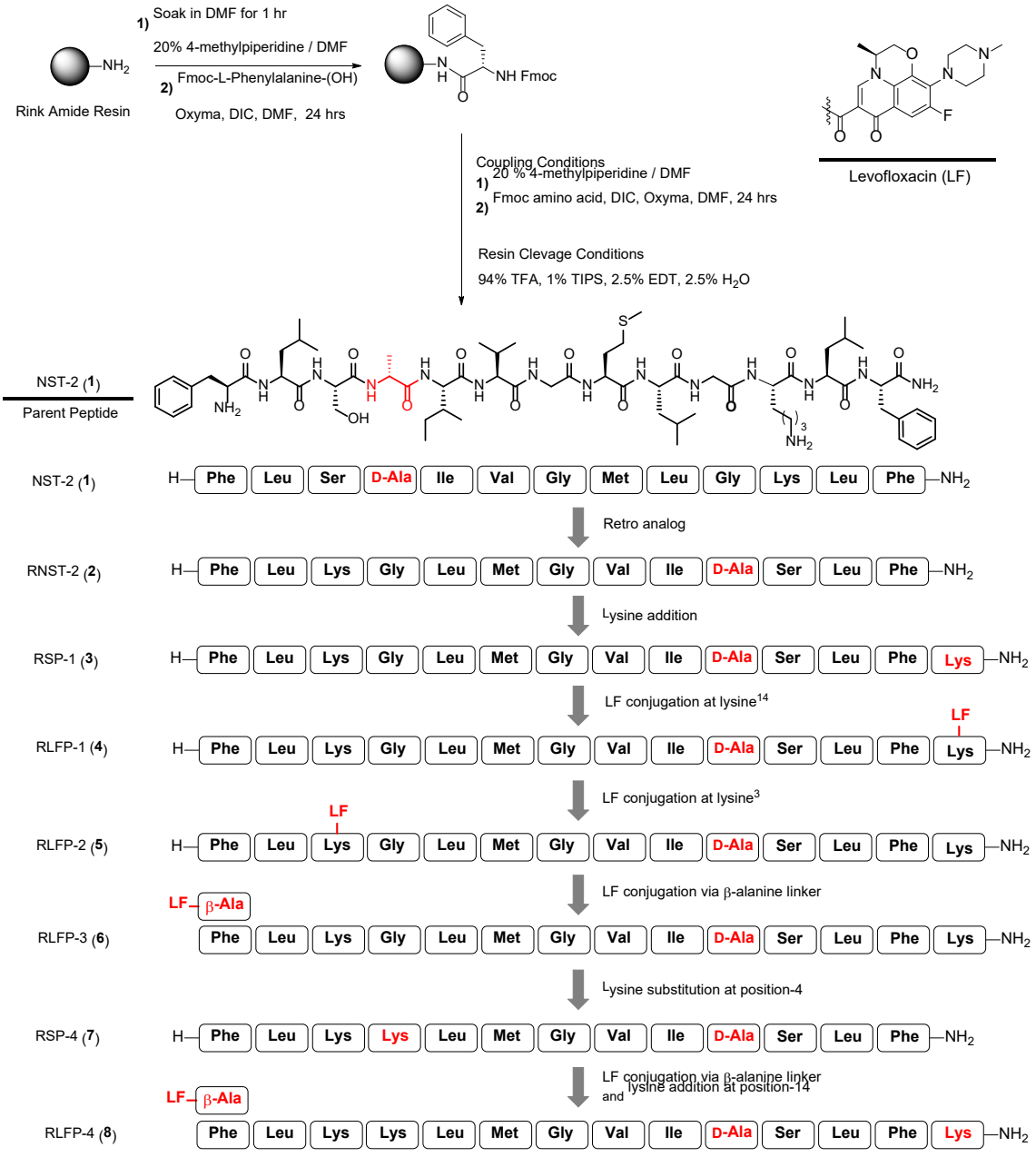

Scheme 1. Synthesis and structure of D-alanine modified NST-2 (**1**), its retro analog **2**, and levofloxacin conjugates.

 doi:10.20944/preprints202411.0510.v1

2.2.2. Mass and NMR Spectroscopic Analysis of Peptides

For the determination of mass of peptides, electrospray ionization with quadrupole time-of-flight mass spectrometery (ESI-QIT-MS) technique was used. All spectra were recorded on Amazon Speed mass spectrometer (Bruker Daltonics). 4500 V electrospray voltage was applied at the spraying needle with 200 °C. Sample was injected with gas flow at 15 psi. All the peptides were also characterized with ^{1}H-NMR and ^{13}C-NMR spectroscopy. The 600 MHz and 800 MHz NMR spectrometer (Bruker) equipped with an Avance III HD console (5 RF channels, 2 receivers), and with a TCI (^{1}H/^{13}C/^{15}N/^{31}P/2H) CryoProbe which is a H-optimized triple resonance NMR 'inverse' probe, and also a RT probe.

2.2.2.1. Synthesis of NST-2 Peptide (1)

The peptide **1** was synthesized by solid phase peptide synthesis (SPPS) method as described earlier [32]. Overall yield: 68.6%; $[\alpha]_D^{24}$= -40 (c 0.22, 60% ACN, 40% H_2O, 0.082% TFA). Purity of the peptide was confirmed with UPLC (Figure S1).

2.2.2.2. Synthesis of RNST-2 Peptide (2)

Reversing the amino acid sequence of peptide **1** via SPPS gave the peptide **2**. Overall yield: 24.63%; $[\alpha]_D^{24}$= -202 (c 0.001, MeOH). UV-Vis. (MeOH) λ_{max} (log ε): 228.0 (1.349) nm. IR (KBr, cm^{-1}): 1054.60 (C-O stretching, CN stretching, NH bending), 1456.81 (C-H bending, Aromatic C=C stretching), 1636.50 (NHC=O stretching), 2927.3 (C-H stretching), 3334.86 (OH stretching) and 3853.15 (NH stretching). ^{1}H NMR (d$_6$-DMSO, 600 MHz): δ_H 0.72–0.81 (18H, m, $(CH_3)_2$–Leu$^{2, 5, 12}$), 0.80–0.87 (12H, m, δ-CH_3–IIe^9, γ-CH_3–IIe^9, $(CH_3)_2$–Val^8), 1.16 (3H, d, CH_3–D-Ala^{10}), 1.29–1.55 (18H, m, CH_2–Leu$^{2, 5, 12}$, δ-CH–Leu$^{2, 5, 12}$), 1.30–2.39 (β-CH–IIe^9, β-CH_2–Met^6, β-CH_2–Lys^3, γ- CH_2–Lys^3, δ-CH_2–Lys^3), 1.45–1.50 (1H, m, γ-CH–IIe^9), 1.92 (1H, m, β-CH–Val^8), 1.99 (1H, m, δ- CH_3–Met^6), 1.78–1.81 (2H, m, γ- CH_2–Met^6), 2.72 (2H, t, Δ- CH_2–Lys^3), 2.85–3.15 (4H, dd, CH_2–Phe$^{1, 13}$), 3.60 (2H, m, CH_2–Ser^{11}), 3.77–3.80 (4H, m, CH_2–Gly^{4,7}), 3.94–4.12 (6H, m, α-CH–Phe^1, α-CH–Leu^2, α-CH–Leu^5, α-CH–Met^6, α-CH–Leu^{12}, α-CH–Phe^{13}), 4.13–4.34 (5H, m, α-CH–Lys^3, α-CH–Val^8, α-CH–IIe^9, α-CH–D-Ala^{10}, α-CH–Ser^{11}), 5.3 (1H, bs, OH–Ser^{11}), 7.16–4.27 (10H, m, CH_{Ar}–phe^{1,13}), 7.74–7.95 (7H, m, NH–Leu^2, NH–Gly^4, NH–Leu^5, NH–Met^6, NH–Val^8, NH–D-Ala^{10}, NH–Leu^{12}). 7.96–8.49 (6H, m, NH–Phe^1, NH–Lys^3, NH–Gly^7, NH–IIe^9, NH–Ser^{11}, NH–Phe^{13}). ^{13}C-NMR (d$_6$-DMSO, 150 MHz): δ ppm 11.17, 11.19, 14.78, 15.40, 18.36, 18.45, 19.36, 21.59, 21.64, 21.73, 21.77, 22.40, 23.10, 23.22, 23.30, 23.35, 24.23, 24.32, 24.80, 26.85, 29.69, 30.63, 31.46, 31.80, 34.63, 36.39, 37.46, 40.62, 40.85, 41.06, 42.07, 42.18, 48.40, 51.33, 52.25, 52.30,52.84, 54.08, 54.84, 54.95, 57.72, 58.03, 61.90, 126.56, 127.33, 128.35, 128.73, 129.26, 129.28, 129.39, 129.74, 137.96, 168.94, 170.11, 170.89, 170.94, 171.00, 171.48, 171.72, 171.92, 171.94, 171.99, 172.36, 172.44, 172.48, 173.36. HRMS (ESI) $[M+Na]^+$ *m/z:* calculated for $[C_{68}H_{111}N_{15}O_{14}S+Na]^+$: 1416.8053; found: 1416.8042.

2.2.2.3. Synthesis of RSP-1 Peptide (3)

The peptide **3** was synthesized by SPPS, wherein lysine was added to position-14 of retro analog **2**. Overall yield: 7.6%; $[\alpha]_D^{24}$= -208.00 (c 0.001, MeOH). UV-Vis. (MeOH) λ_{max} (log ε): 228.0 (1.349) nm. IR (KBr, cm^{-1}): 1143.30, 1201.2 (C-O stretching, CN stretching, NH bending), 1472.84 (C-H bending, Aromatic C=C stretching), 1635.72 (NHC=O stretching), 2981.04 (C-H stretching), 3356.37 (OH, NH stretching). ^{1}H NMR (d$_6$-DMSO, 600 MHz): δ_H 0.72–0.87 (18H, m, $(CH_3)_2$–Leu$^{2, 5, 12}$), 0.80–0.87 (12H, m, δ-CH_3–IIe^9, γ-CH_3–IIe^9, $(CH_3)_2$–Val^8), 1.16 (3H, d, CH_3–D-Ala^{10}), 1.29–1.55 (18H, m, CH_2–Leu$^{2, 5, 12}$, δ-CH–Leu$^{2, 5, 12}$), 1.30–2.39 (β-CH–IIe^9, β-CH_2–Met^6, β-CH_2–Lys$^{3, 14}$, γ- CH_2–Lys$^{3, 14}$, δ-CH_2–Lys$^{3, 14}$), 1.45–1.50 (1H, m, γ-CH–IIe^9), 1.92 (1H, m, β-CH–Val^8), 1.99 (1H, m, δ- CH_3–Met^6), 1.78–1.81 (2H, m, γ- CH_2–Met^6), 2.72 (2H, t, Δ- CH_2–Lys$^{3, 14}$), 2.85–3.15 (4H, dd, CH_2–Phe$^{1, 13}$), 3.60 (2H, m, CH_2–Ser^{11}), 3.77–3.80 (4H, m, CH_2–Gly^{4,7}), 4.04–4.20 (4H, m, α-CH–Phe^1, α-CH–Leu^5, α-CH–Val^8, α-CH–IIe^9,), 4.13–4.34 (8H, m, α-CH–Leu^2, α-CH–Lys^3, α-CH–Met^6, α-CH–D-Ala^{10}, α-CH–Ser^{11}, α-CH–Leu^{12}, α-CH–Phe^{13}, α-CH–Lys^{14}), 5.3 (1H, bs, OH–Ser^{11}), 7.16–4.27 (10H, m, CH_{Ar}–phe^{1,13}), 7.84–8.10 (8H, m, NH–Leu^5, NH–Gly^7, NH–Val^8, NH–IIe^9, NH–D-Ala^{10}, NH–Ser^{11}, NH–Leu^{12}, NH–Phe^{13}). 8.11–8.60 (5H, m, NH–Leu^2, NH–

 doi:10.20944/preprints202411.0510.v1

Lys[3], NH–Gly[4], NH–Met[6], NH–Lys[14]). ^{13}C-NMR (d$_6$-DMSO, 150 MHz): δ ppm 11.05, 15.25, 15.34, 18.12, 18.20, 19.21, 19.36, 21.44, 21.46, 21.51, 21.60, 21.70, 22.21, 22.34, 22.98, 23.00, 23.04, 23.08, 23.14, 23.19, 23.93, 24.03, 24.12, 24.53, 24.57, 26.60, 26.69, 27.15, 28.12, 29.52, 30.30, 31.47, 30.52, 31.40, 34.36, 37.10, 37.88, 38.69, 40.27, 40.83, 40.94, 41.83, 48.10, 49.17, 49.26, 51.01, 51.18, 52.54, 53.27, 57.72, 61.70, 126.29, 126.42, 127.14, 127.58, 127.81, 128.06, 128.19, 128.29, 128.52, 129.12, 129.60, 134.96, 137.65, 168.57, 169.14, 170.13, 170.62, 170.77, 170.88, 171.10, 171.51, 171.69, 171.72. HRMS (ESI) $[M+Na]^+$ *m/z:* calculated for $[C_{74}H_{123}N_{17}O_{15}S+Na]^+$: 1544.9003; found: 1544.8978.

2.2.2.4. Synthesis of RLFP-1 (4)

The peptide **4** was synthesized by SPPS, wherein lysine was added to the retro analog **2** followed by its conjugation with levofloxacin. Overall yield: 22.5%; $[\alpha]_D^{24}$= 22.5%; $[\alpha]_D^{24}$= +120 (c 0.001, MeOH). UV-Vis. (MeOH) λ_{max} (log ε): 206.0 (1.064) nm. IR (KBr, cm^{-1}): 1196.40 (C-O stretching, CN stretching, NH bending), 1455.64 (C-H bending, Aromatic C=C stretching), 1635.96 (NHC=O stretching), 2981.07 (C-H stretching), 3335.69 (OH, NH stretching). ^{1}H NMR (d$_6$-DMSO, 600 MHz): δ_H 0.72–0.81 (18H, m, $(CH_3)_2$–Leu[2, 5, 12]), 0.80–0.87 (12H, m, δ-CH$_3$–IIe[9], γ-CH$_3$–IIe[9], $(CH_3)_2$–Val[8]), 1.16 (3H, d, CH$_3$–D-Ala[10]), 1.29–1.55 (21H, m, 14′-CH$_3$–LF, α-CH$_2$–*b*Ala CH$_2$–Leu[2, 5, 12], δ-CH–Leu[2, 5, 12]), 1.30–2.39 (β-CH–IIe[9], β-CH$_2$–Met[6], β-CH$_2$–Lys[3,14], γ- CH$_2$–Lys[3,14], δ-CH$_2$–Lys[3,14]), 1.45–1.50 (1H, m, γ-CH–IIe[9]), 1.92 (1H, m, β-CH–Val[8]), 1.99 (1H, m, δ- CH$_3$–Met[6]), 1.78–1.81 (2H, m, γ- CH$_2$–Met[6]), 2.72 (6H, t, Δ- CH$_2$–Lys[3,14]), 2.85–3.16 (11H, dd, 15′-CH$_3$–LF, CH$_2$–Phe[1, 13], 3′′ 5′′-CH$_2$–LF), 3.47 (2′′ 6′′-CH$_2$–LF), 3.60 (2H, m, CH$_2$–Ser[11]), 3.68–3.77 (4H, m, CH$_2$–Gly[4,7]), 4.04–4.18 (5H, m, α-CH–Phe[1], α-CH–Lys[3], α-CH–Leu[5], α-CH–Val[8], α-CH–IIe[9]), 4.22–4.54 (11H, m, α-CH–Leu[2], α-CH–Met[6], α-CH–D-Ala[10], α-CH–Ser[11], , α-CH–Leu[12], α-CH–Phe[13], α-CH–Lys[14], 2′-CH$_2$–LF), 4.84 (3′-CH–LF), 5.3 (1H, bs, OH–Ser[11]), 7.16–7.27 (10H, m, CH$_{Ar}$–phe[1,13]), 7.53 (1H, **8′**-CH–LF), 7.75–8.00 (8H, m, NH–Lys[3], NH–Leu[5], NH–Met[6], NH–Val[8], NH–D-Ala[10], NH–Ser[11], NH–Leu[12], NH–Phe[13]). 8.01–8.58 (6H, m, NH–Phe[1], NH–Leu[2], NH–Gly[4], NH–Gly[7], NH–IIe[9], NH–Lys[14]), 8.76 (1H, **5′**-CH–LF). ^{13}C-NMR (d$_6$-DMSO, 150 MHz): δ ppm 14.7, 15.4, 15.5, 18.3, 19.3, 19.3, 21.6, 21.7, 21.7, 21.8, 22.4, 22.7, 22.8, 23.1, 23.2, 23.3, 24.1, 24.2, 24.3, 24.7, 26.8, 27.3, 29.2, 29.2, 29.7, 30.6, 30.6, 31.0, 31.5, 31.7, 34.6, 36.1, 36.4, 37.1, 38.9, 40.3, 40.8, 41.0, 42.0, 42.1, 48.8, 51.3, 51.4, 52.3, 52.8, 53.3, 57.7, 58.0, 61.8, 64.4, 73.0, 129.3, 129.3, 129.4, 129.7, 133.9, 134.8, 137.7, 156.2, 162.8, 167.9, 168.9, 171.0, 171.4, 171.7, 171.8, 171.9, 172.5, 173.8. HRMS (ESI) $[M+H]^+$ *m/z:* calculated for $[C_{92}H_{141}FN_{20}O_{18}S+H]^+$: 1866.0516; found: 1866.1101.

2.2.2.5. Synthesis of RLFP-2 Peptide (5)

The peptide **5** was synthesized by SPPS, wherein lysine was added to the retro analog **2** followed by levofloxacin conjugation with lysine-3. Overall yield: 17%; $[\alpha]_D^{24}$= +5 (c 0.001, MeOH). UV-Vis. (MeOH) λ_{max} (log ε): 206 (1.064) nm. IR (KBr, cm^{-1}): 1145.49 (C-O stretching, CN stretching, NH bending), 1456.10 (C-H bending, Aromatic C=C stretching), 1627.49 (NHC=O stretching), 2981.05 (C-H stretching), 3285.26 (OH, NH stretching). ^{1}H NMR (d$_6$-DMSO, 600 MHz): δ_H 0.72–0.81 (18H, m, $(CH_3)_2$–Leu[2, 5, 12]), 0.80–0.87 (12H, m, δ-CH$_3$–IIe[9], γ-CH$_3$–IIe[9], $(CH_3)_2$–Val[8]), 1.16 (3H, d, CH$_3$–D-Ala[10]), 1.29–1.55 (21H, m, 14′-CH$_3$–LF, CH$_2$–Leu[2, 5, 12], δ-CH–Leu[2, 5, 12]), 1.30–2.39 (β-CH–IIe[9], β-CH$_2$–Met[6], β-CH$_2$–Lys[3,14], γ- CH$_2$–Lys[3,14], δ-CH$_2$–Lys[3,14]), 1.45–1.50 (1H, m, γ-CH–IIe[9]), 1.92 (1H, m, β-CH–Val[8]), 1.99 (1H, m, δ- CH$_3$–Met[6]), 1.78–1.81 (2H, m, γ- CH$_2$–Met[6]), 2.72 (2H, t, Δ- CH$_2$–Lys[3,14]), 2.85–3.16 (11H, dd, 15′-CH$_3$–LF, CH$_2$–Phe[1, 13], 3′′ 5′′-CH$_2$–LF), 3.47 (2′′ 6′′-CH$_2$–LF), 3.60 (2H, m, CH$_2$–Ser[11]), 3.68–3.77 (4H, m, CH$_2$–Gly[4,7]), 4.07–4.21 (5H, m, α-CH–Lys[3], α-CH–Val[8], α-CH–IIe[9], α-CH–Leu[12], α-CH–Lys[14]), 4.22–4.54 (11H, m, α-CH–Phe[1], α-CH–Leu[2], α-CH–Leu[5], α-CH–Met[6], α-CH–D-Ala[10], α-CH–Ser[11], α-CH–Phe[13] 2′-CH$_2$–LF), 4.84 (3′-CH–LF), 5.3 (1H, bs, OH–Ser[11]), 7.16–4.27 (10H, m, CH$_{Ar}$–phe[1,13]), 7.53 (1H, **8′**-CH–LF), 7.83–8.00 (7H, m, NH–Lys[3], NH–Leu[5], NH–Met[6], NH–Val[8], NH–IIe[9], NH–D-Ala[10], NH–Phe[13]). 8.01–8.56 (7H, m, NH–Phe[1], NH–Leu[2], NH–Gly[4], NH–Gly[7], NH–Ser[11], NH–Leu[12], NH–Lys[14]), 8.76 (1H, **5′**-CH–LF). ^{13}C-NMR (d$_6$-DMSO, 150 MHz): δ ppm 15.01, 15.64, 15.80, 18.09, 18.73, 19.55, 21.82, 21.88, 21.95, 22.04, 22.65, 22.74, 23.06, 23.35, 23.48, 2..54, 23.68, 24.40, 24.50, 24.61, 25.13, 26.91, 27.53, 29.52, 29.99, 30.66, 30.68, 31.45, 31.64, 31.85, 34.93, 36.45, 37.34, 37.39, 40.39, 40.54, 40.54, 40.78, 41.05, 42.56, 43.22, 47.80, 48.96, 51.78, 51.91, 52.33, 52.51, 52.87, 52.99, 53.62, 53.73, 54.04, 54.80, 55.65, 58.35, 58.78, 61.89, 64.84, 73.52, 116.77, 117.58, 118.25, 119.73, 127.03, 127.83, 128.73, 128.75, 129.11,

 doi:10.20944/preprints202411.0510.v1

129.61, 130.05, 134.07, 134.88, 137.85, 141.16, 156.78, 159.07, 159.23, 159.38, 159.54, 168.29, 169.62, 169.73, 170.55, 171.16, 171.45, 171.59, 171.80, 172.11, 172.37, 172.87, 172.91, 173.20, 173.83, 174.38. LRMS (ESI) *m/z*: 1912.3 $[M+2Na+H]^+$

2.2.2.6. Synthesis of RLFP-3 (6)

The peptide **6** was synthesized by SPPS, wherein lysine was added to retro analog **2** followed by levofloxacin conjugation with its phenylalanine-1 via β-alanine linker. Overall yield: 21%; $[\alpha]_D^{24}$= -45 (c 0.001, MeOH). UV-Vis. (MeOH) λ_{max} (log ε): 224 (1.064) nm. IR (KBr, cm^{-1}): 1135.15 (C-O stretching, CN stretching, NH bending), 1456.85 (C-H bending, Aromatic C=C stretching), 1670.12 (NHC=O stretching), 2972.69 (C-H stretching), 3648.95 (OH, NH stretching). ^{1}H NMR (d$_6$-DMSO, 600 MHz): δ_H 0.72–0.81 (18H, m, $(CH_3)_2$–Leu$^{2, 5, 12}$), 0.80–0.87 (12H, m, δ-CH_3–IIe^9, γ-CH_3–IIe^9, $(CH_3)_2$–Val^8), 1.16 (3H, d, CH_3–D-Ala^{10}), 1.29–1.55 (21H, m, 14′-CH_3–LF, CH_2–Leu$^{2, 5, 12}$, δ-CH–Leu$^{2, 5, 12}$), 1.30–2.39 (β-CH–IIe^9, β-CH_2–Met^6, β-CH_2–Lys^{3,14}, γ- CH_2–Lys^{3,14}, δ-CH_2–Lys^{3,14}), 1.45–1.50 (1H, m, γ-CH–IIe^9), 1.92 (1H, m, β-CH–Val^8), 1.99 (1H, m, δ- CH_3–Met^6), 1.78–1.81 (2H, m, γ- CH_2–Met^6), 2.35 (α-CH_2–*b*Ala), 2.72 (2H, t, Δ- CH_2–Lys^{3,14}), 2.85–3.16 (11H, dd, 15′-CH_3–LF, CH_2–Phe$^{1, 13}$, 3′′ 5′′-CH_2–LF), 3.37–3.44 (β-CH_2–Ala), 3.47 (2′′ 6′′-CH_2–LF), 3.60 (2H, m, CH_2–Ser^{11}), 3.66–3.80 (4H, m, CH_2–Gly^{4,7}), 4.11–4.23 (5H, m, α-CH–Lys^3, α-CH–Val^8, α-CH–IIe^9, α-CH–Leu^{12}, α-CH–Lys^{14}), 4.23–4.55 (12H, m, α-CH–Phe^1, α-CH–Leu^2, α-CH–Leu^5, α-CH–Met^6, α-CH–D-Ala^{10}, α-CH–Ser^{11}, α-CH–Phe^{13}, 2′-CH_2–LF), 4.84 (3′-CH–LF), 5.3 (1H, bs, OH–Ser^{11}), 7.16–7.27 (10H, m, CH_{Ar}–phe^{1,13}), 7.53 (1H, **8′**-CH–LF), 7.85–8.00 (8H, m, NH–Leu^2, NH–Lys^3, NH–Val^8, NH–IIe^9, NH–Ser^{11}, NH–Leu^{12}, NH–Phe^{13}, NH–Lys^{14}). 8.01–8.31 (6H, m, NH–Phe^1, NH–Gly^4, NH–Leu^5, NH–Met^6, NH–Gly^7, NH–D-Ala^{10}), 8.76 (1H, **5′**-CH–LF), 9.88 (NH–*b*Ala). ^{13}C-NMR (d$_6$-DMSO, 150 MHz): δ ppm 11.01, 14.58, 15.22, 17.9, 18.14, 18.39, 19.16, 21.40, 21.43, 21.55, 22.09, 22.18, 22.30, 22.96, 23.12, 23.29, 24.01, 24.07, 24.51, 26.61, 26.64, 29.48, 30.52, 31.30, 31.42, 31.81, 31.92, 35.29, 36.37, 37.11, 37.53, 38.70, 38.76, 40.19, 40.56, 40.81, 41.79, 41.89, 42.47, 48.01, 50.93, 51.11, 51.59, 51.98, 52.21, 52.30, 53.35, 53.75, 53.91, 53.95, 54.63, 57.27, 57.60, 61.68, 68.35, 126.28, 127.93, 128.01, 128.07, 129.13, 129.19, 137.59, 137.81, 168.47, 168.52, 169.29, 170.20, 170.57, 170.70, 170.98, 171.08, 171.29, 171.63, 171.91, 172.07, 173.20, 173.24. HRMS (ESI) $[M+Na]^+$ *m/z:* calculated for $[C_{95}H_{146}FN_{21}O_{19}S+Na+H]^+$: 1960.0785; found: 1960.0653.

2.2.2.7. Synthesis of RSP-4 Peptide (7)

The peptide **7** was prepared by SPPS, wherein glycine-4 of retro analog **2** was substituted with lysine. Overall yield: 28%; $[\alpha]_D^{24}$= +88 (c 0.001, MeOH). UV-Vis. (MeOH) λ_{max} (log ε): 230.0 (1.979) nm. ^{1}H NMR (d$_6$-DMSO, 600 MHz): δ_H 0.72–0.87 (18H, m, $(CH_3)_2$–Leu$^{2, 5, 12}$), 0.80–0.87 (12H, m, δ-CH_3–IIe^9, γ-CH_3–IIe^9, $(CH_3)_2$–Val^8), 1.16 (3H, d, CH_3–D-Ala^{10}), 1.29–1.55 (18H, m, CH_2–Leu$^{2, 5, 12}$, δ-CH–Leu$^{2, 5, 12}$), 1.30–2.39 (β-CH–IIe^9, β-CH_2–Met^6, β-CH_2–Lys$^{3, 4}$, γ- CH_2–Lys$^{3, 4}$, δ-CH_2–Lys$^{3, 4}$), 1.45–1.50 (1H, m, γ-CH–IIe^9), 1.92 (1H, m, β-CH–Val^8), 1.99 (1H, m, δ- CH_3–Met^6), 1.78–1.81 (2H, m, γ- CH_2–Met^6), 2.72 (2H, t, Δ- CH_2–Lys$^{3, 4}$), 2.85–3.15 (4H, dd, CH_2–Phe$^{1, 13}$), 3.60 (2H, m, CH_2–Ser^{11}), 3.77–3.80 (4H, m, CH_2–Gly^7), 4.04–4.22 (5H, m, α-CH–Phe^1, α-CH–Lys^4, α-CH–Leu^5, α-CH–Val^8, α-CH–IIe^9,), 4.23–4.39 (7H, m, α-CH–Leu^2, α-CH–Lys^3, α-CH–Met^6, α-CH–D-Ala^{10}, α-CH–Ser^{11}, α-CH–Leu^{12}, α-CH–Phe^{13}), 5.3 (1H, bs, OH–Ser^{11}), 7.16–4.27 (10H, m, CH_{Ar}–phe^{1,13}), 7.84–8.00 (7H, m, NH– Lys^4, NH–Leu^5, NH–Val^8, NH–IIe^9, NH–D-Ala^{10}, NH–Leu^{12}, NH–Phe^{13}). 8.01–8.60 (5H, m, NH–Leu^2, NH–Lys^3, NH–Met^6, NH–Gly^7, NH–Ser^{11}). ^{13}C-NMR (d$_6$-DMSO, 150 MHz): δ ppm 14.62, 15.25, 18.08, 18.13, 18.45, 19.28, 21.36, 21.45, 21.70, 22.14, 22.32, 22.94, 23.14, 24.05, 24.14, 24.55, 24.59, 26.69, 26.74, 27.17, 28.12, 29.37, 30.30, 30.58, 31.31, 31.37, 32.05, 34.37, 37.09, 37.31, 38.75, 39.07, 39.20, 39.34, 39.49, 39.62, 39.76, 39.90, 40.02, 40.48, 41.07, 41.93, 43.29, 48.16, 50.99, 51.15, 51.87, 52.04, 52.23, 52.40, 53.26, 53.86, 54.00, 57.68, 61.79, 126.27, 126.30, 126.42, 127.16, 128.11, 128.19, 128.53, 129.11, 129.16, 129.61, 134.90, 137.88, 167.97, 170.73, 171.29, 171.31, 171.51, 171.63, 171.66, 172.07. HRMS (ESI) $[M+Na]^+$ *m/z:* calculated for $[C_{72}H_{120}N_{16}O_{14}S+Na]^+$: 1487.8788; found: 1487.8763.

2.2.2.8. Synthesis of RLFP-4 Peptide (8)

 doi:10.20944/preprints202411.0510.v1

The peptide **8** was synthesized by SPPS, wherein glycine-4 of retro analog **2** was substituted with lysine followed levofloxacin conjugation at phenylalanine-1 via β-alanine linker. Overall yield: 25%; $[\alpha]_D^{24}$= +131.5 (c 0.001, MeOH). UV-Vis. (MeOH) λ_{max} (log ε): 225.0 (1.65) nm. ^{1}H NMR (d$_6$-DMSO, 600 MHz): δ_H 0.75–0.85 (18H, m, $(CH_3)_2$–Leu^{2,5,12}), 0.78–0.83 (12H, m, δ-CH_3–IIe^9, γ-CH_3–IIe^9, $(CH_3)_2$–Val^8), 1.16 (3H, d, CH_3–D-Ala^{10}), 1.26–1.61 (21H, m, 14′-CH_3–LF, CH_2–Leu^{2,5,12}, δ-CH–Leu^{2,5,12}), 1.30–2.39 (β-CH–IIe^9, β-CH_2–Met^6, β-CH_2–Lys^{3,4}, γ- CH_2–Lys^{3,4}, δ-CH_2–Lys^{3,4}), 1.45–1.50 (1H, m, γ-CH–IIe^9), 1.92 (1H, m, β-CH–Val^8), 2.00 (1H, m, δ- CH_3–Met^6), 1.78–1.81 (2H, m, γ- CH_2–Met^6), 2.35 (α-CH_2–*b*Ala), 2.72 (2H, t, Δ- CH_2–Lys^{3,4}), 2.85–3.16 (11H, dd, 15′-CH_3–LF, CH_2–Phe^{1,13}, 3′ 5′-CH_2–LF), 3.37–3.44 (β-CH_2–*b*Ala), 3.47 (2′ 6′-CH_2–LF), 3.61–3.85 (2H, m, CH_2–Ser^{11}), 3.66–3.84 (4H, m, CH_2–Gly^7), 4.09–4.22 (4H, m, α-CH–Lys^4, α-CH–Leu^5, α-CH–IIe^9, α-CH–Leu^{12},), 4.23–4.54 (8H, m, α-CH–Phe^1, α-CH–Leu^2, α-CH–Lys^3, α-CH–Met^6, α-CH–Val^8, α-CH–D-Ala^{10}, α-CH–Ser^{11}, α-CH–Phe^{13}, 2′ 6′-CH_2–LF), 4.84 (3′-CH–LF), 5.3 (1H, bs, OH–Ser^{11}), 7.16–7.27 (10H, m, CH_{Ar}–phe^{1,13}), 7.53 (1H, **8′**-CH–LF), 7.80–8.03 (8H, m, NH–Lys^3, NH–Lys^4, NH–Met^6, NH–Val^8, NH–IIe^9, NH–D-Ala^{10}, NH–Ser^{11}, NH–Leu^{12}). 8.04–9.88 (6H, m, NH–Phe^1, NH–Leu^2, NH–Leu^5, NH–Gly^7, NH–Phe^{13}), 8.76 (1H, **5′**-CH–LF), 9.88 (NH–*b*Ala). ^{13}C-NMR (d$_6$-DMSO, 150 MHz): δ ppm 10.98, 14.57, 15.19, 17.89, 18.05, 18.39, 19.15, 21.38, 21.41, 21.59, 22.11, 22.15, 22.17, 22.21, 22.89, 23.05, 23.09, 23.26, 23.98, 24.06, 24.08, 24.50, 26.62, 26.64, 29.30, 30.55, 31.26, 32.03, 34.92, 35.30, 36.30, 37.21, 37.29, 40.42, 40.60, 41.81, 42.45, 47.30, 47.97, 50.92, 51.13, 51.90, 52.14, 52.19, 5333, 53.71, 53.92, 54.40, 57.26, 57.52, 61.74, 68.32, 124.22, 126.09, 126.20, 127.92, 128.02, 129.02, 129.06, 137.77, 137.82, 145.01, 163.90, 168.46, 170.45, 170.53, 170.99, 171.18, 171.20, 171.25, 171.51, 171.92, 171.97, 172.88, 173.93, 173.94. HRMS (ESI) $[M+Na]^+$ *m/z:* calculated for $[C_{93}H_{143}FN_{20}O_{18}S+Na+H]^+$: 1903.0570; found: 1903.0484.

2.2.3. Circular Dichroism (CD) and Secondary Structure Analysis

The far-ultraviolet circular dichroism (CD) spectra were recorded using a JASCO J-810 spectropolarimeter (Jasco, Tokyo, Japan), with measurements taken in a quartz cuvette with a 10 mm path length. The temperature was kept at 22 °C, and the instrument was calibrated with D-(+)-10-camphorsulfonic acid. Peptides were dissolved in 20 mM SDS to a final concentration of 15 μM. The CD spectra were collected over a wavelength range of 190 to 260 nm with a bandwidth of 2 nm. Each spectrum was recorded with ten consecutive scans at a rate of 50 nm/min, and the baseline was obtained under identical conditions. Secondary structures, i.e., percentage of alpha-helix and other secondary structures, were quantified from CD data using Bestsel software (https://bestsel.elte.hu/index.php).

2.3. Biological Studies

2.3.1. Antibacterial Assay

The antibacterial activity of peptide analogues was tested against different bacterial strains, i.e., *Staphylococcus aureus* (NCTC 13277), *Bacillus subtilis* (ATCC 23857), *Escherichia coli* (ATCC 25922), *Salmonella typhi* (ATCC 14028), and *Pseudomonas aeruginosa* (ATCC 10145). These strains were obtained from the microbial bank of Dr. Panjwani Center for Molecular Medicine and Drug research (PCMD), International Center for Chemical and Biological Sciences (ICCBS), University of Karachi. Colonies of these bacterial strains were grown in respective agar media, then inoculated in Mueller Hinton (MH) broth (Oxoid, UK) and incubated at 37 °C for overnight. The peptide solutions were first diluted 1 in 100 (from stock solution at 20 mM) and then further two-fold dilution in MH broth in sterile 96-well plate were performed, resulting in 100 μL broth containing increasing concentration: of analogs. Bacteria in their exponential growth phase were diluted in MH broth, and 100 μL of this suspension was added in each well. This resulted in a final 200 μL suspension containing 0.5-1.0 X 10^6 CFU/mL. Then, these plates were incubated at 37°C for 20–22 h. MIC (Minimum Inhibitory Concentration) values were determined as the concentrations of peptides causing >99% inhibition of bacterial growth.

2.3.2. Antifungal Assay

 doi:10.20944/preprints202411.0510.v1

Candida albicans (ATCC 36082) was cultured on Sabourad Dextrose Agar (SDA). A single colony was inoculated in Sabouraud Dextrose Broth (SDB) medium and grown overnight at 37 °C while shaking. The next day, susceptibility of *C. albicans* was tested using broth microdilution assay. Peptide analogues were diluted in SDB media by two-fold, resulting in 100 µL medium containing increasing concentrations of analogs. The overnight culture (turbidity at OD_{600} = 1) was 1000x diluted in SDB. Then 100 µL of this suspension was added to each well, resulting in a final 200 µL suspension containing 2–4 x 10^5 CFU/mL. The plate was incubated at 37°C for 24 h. The next day, MIC (Minimum Inhibitory Concentration) values were determined as the concentrations of peptides causing >99% inhibition of yeast growth.

2.3.3. Antiproliferative Assay

Human breast cancer (MCF-7) and human cervical cancer (HeLa) cells were obtained from the cell culture bank of PCMD in ICCBS, University of Karachi. These cells were maintained in Dulbecco's Modified Eagle Medium (DMEM) supplemented with 10% fetal bovine serum, and incubated at 37 °C and 5 % CO_2. The antiproliferative activity of samples were determined by MTT assay. Briefly, the cells were washed with PBS and trypsinized. After determination of the cell number using Malassez cell counting, 100 µL of cell suspension were seeded in 96-well plate at the density of 6,000 cells/well and incubated at 37 °C and 5% CO_2. After 24 h, the cells were treated with increasing concentrations of analogs. The next day, media was removed and 200 µL of MTT dye (0.5 mg/mL) was added in each well and incubated for 3 h at 37°C in 5% CO_2 incubator. Then media was removed and 100 µL DMSO was added to solubilize formazan crystals. After one minute of shaking, the absorbance was recorded at 540 nm in microplate reader (Multiskan GO, ThermoScientific). Finally, percent inhibition of proliferation was calculated using the following formula:

$$\% \text{ inhibition of proliferation} = \frac{\text{O.D of treated well} - \text{O.D of media control}}{\text{O.D of untreated control} - \text{O.D of media control}} \times 100$$

2.3.4. Hemolytic Assay

For hemolytic assay, fresh human blood (2 mL) was obtained from healthy donor in EDTA tube while following the protocol of approval from Independent Ethics Committee of ICCBS (Approval number ICCBS/IEC-047-HB-2019/Protocol/1.0). The blood was centrifuged and upper supernatant plasma was removed. The cell pellets were washed with sterile PBS for three times. The washed blood cells were then diluted 25 times to make 4% concentration of initial blood cells. Red blood cells (500 µL) were treated with increasing concentrations of analogs, triton X-100 at 0.1 % being used as positive control giving 100% hemolysis. After 1 h incubation at 37°C, tubes were centrifuged at 800 rpm for 5 min to pellet down red blood cells. After centrifugation, 200 µL of supernatant were transferred into 96 well plate and absorbance was recorded at 576 nm using microplate reader (MultiSkan Go, ThermoScientific).

Then following formula was applied to calculate percent hemolysis:

$$\% \text{ Hemolysis} = \frac{\text{O.D of test sample} - \text{O.D of PBS control}}{\text{O.D of Tritox X positive control} - \text{O.D of PBS control}} \times 100$$

2.3.5. Atomic Force Microscopy (AFM) Imaging

Different bacteria (*S. typhi, E. coli*, and *P. aeruginosa*) adjusted to 2–3×10^7 CFU/mL were treated with 2XMIC values of analogs and incubated overnight at 37°C. The next day, bacteria were washed, dispersed in sterile pure grade water, dispensed in poly-L-lysine coated mica slides, and left for air drying. Changes in the morphology of bacteria were studied with atomic force microscope (Agilent 5500, Chandler, AZ, USA). The whole analysis was done in tapping mode. Images were collected and optimized at scans velocity of 1–5 µm/s and 512 × 512-line resolution and processed through PicoView 1.2 imaging software.

3. Results

 doi:10.20944/preprints202411.0510.v1

Lysine enriched peptides are known to possess strong antimicrobial activities with less toxicity towards eukaryotic cells [35–37]. Hence, we decided to investigate the role of lysine using two approaches — addition and substitution — in retro analog of NST-2 peptide. Briefly, L-lysine was added to retro analog **2** at position-14, which afforded RSP-1 peptide (**3**). In addition, glycine at position-4 in the retro analog was substituted with lysine to give RSP-4 peptide (**7**). In the next phase, antibacterial levofloxacin was selected for direct conjugation with the side chain of lysine-14 and lysine-3 of analog **3** to afford RLFP-1 (**4**) and RLPF-2 (**5**), respectively. Similarly, levofloxacin was also conjugated to analog **3** and analog **7** at phenylalanine-1 via β-alanine linker to get RLFP-3 (**6**) and RLFP-4 (**8**), respectively. Amino acid sequences of the peptides (**1–8**) are shown in Table 1. All the peptides were purified with RP-HPLC (PuriFlash®) using PFB15C18XS-250/212 column, and eluted at a flow rate of 3 mL/min by 0.1% TFA in H_2O/ACN (40:60). Their purity was established by UPLC (Agilent 1260 Infinity Diode Array, C-4 reversed-phase analytical column, 5 µm, 150 × 4.6 mm, Santa Clara, CA, USA). Furthermore, 1D / 2D NMR, UV-Vis., FT-IR spectroscopy, polarimetry and HR-MS-ESI mass spectrometry were employed to characterize the peptides. Physiochemical parameters of the synthesized peptides showing the molecular weights, optical rotation and retention time are shown in Table 2.

Table 1. Amino acid sequence of peptides (**1–8**) with changes shown in red color (R = reverse sequence, LF = Levofloxacin, *β*-Ala = beta alanine).

Peptide name	Systematic name	Sequence
NST-2 (**1**)	[G4a]-SHa	H-Phe^1-Leu^2-Ser^3-D-Ala^4-Ile^5-Val^6-Gly^7-Met^8-Leu^9-Gly^{10}-Lys^{11}-Leu^{12}-Phe^{13}-NH_2
RNST-2 (**2**)	R[G4a]-SHa	H-Phe^1-Leu^2-Lys^3-Gly^4-Leu^5-Met^6-Gly^7-Val^8-Ile^9-D-Ala^{10}-Ser^{11}-Leu^{12}-Phe^{13}-NH_2
RSP-1 (**3**)	RNST-2-14K	H-Phe^1-Leu^2-Lys^3- Gly^4-Leu^5-Met^6-Gly^7-Val^8-Ile^9-D-Ala^{10}-Ser^{11}-Leu^{12}-Phe^{13}-Lys^{14}-NH_2
RLFP-1 (**4**)	RRNST-2-14K-14LF	H-Phe^1-Leu^2-Lys^3- Gly^4-Leu^5-Met^6-Gly^7-Val^8-Ile^9-D-Ala^{10}-Ser^{11}-Leu^{12}-Phe^{13}-Lys^{14}(LF)-NH_2
RLFP-2 (**5**)	RNST-2-14K-3LF	H-Phe^1-Leu^2-Lys^3(LF)-Gly^4-Leu^5-Met^6-Gly^7-Val^8-Ile^9-D-Ala^{10}-Ser^{11}-Leu^{12}-Phe^{13}-Lys^{14}-NH_2
RLFP-3 (**6**)	RNST-2-14K-1LF	LF-β-Ala-Phe^1-Leu^2-Lys^3- Gly^4-Leu^5-Met^6-Gly^7-Val^8-Ile^9-D-Ala^{10}-Ser^{11}-Leu^{12}-Phe^{13}-Lys^{14}-NH_2
RSP-4 (**7**)	RNST-2-G4K	H-Phe^1-Leu^2-Lys^3-Lys^4-Leu^5-Met^6-Gly^7-Val^8-Ile^9-D-Ala^{10}-Ser^{11}-Leu^{12}-Phe^{13}-NH_2
RLFP-4 (**8**)	RNST-2-G4K-1LF	LF-β-Ala-Phe^1-Leu^2-Lys^3- Lys^4-Leu^5-Met^6-Gly^7-Val^8-Ile^9-D-Ala^{10}-Ser^{11}-Leu^{12}-Phe^{13}-NH_2

Table 2. Physiochemical parameters of the synthesized peptide analogs showing molecular weights, optical rotation and retention time of each compound obtained from UPLC.

Peptide Name	Chemical Formula	Exact Mass	Observed Mass *	Time(R) **	$[\alpha]_D^{25}$ ‡	Yield §
RNST-2 (**2**)	$C_{68}H_{111}N_{15}O_{14}S$	1393.8	1395.8 $[M+H]^+$	3.1	-202	25
RSP-1 (**3**)	$C_{74}H_{123}N_{17}O_{15}S$	1521.9	1523.9 $[M+H]^+$	2.9	-15	8
RLFP-1 (**4**)	$C_{92}H_{141}FN_{20}O_{18}S$	1865.0	1863.5 $[M+H]^+$	3.3	+120	22
RLFP-2 (**5**)	$C_{92}H_{141}FN_{20}O_{18}S$	1865.0	1912.3 $[M+2Na]^{2+}$	3.7	+5	17
RLFP-3 (**6**)	$C_{95}H_{146}FN_{21}O_{19}S$	1936.0	1936.9 $[M+H]^+$	3.6	-45	26
RSP-4 (**7**)	$C_{72}H_{120}N_{16}O_{14}S$	1464.9	1467.0 $[M+H]^+$	3.1	+88	28
RLFP-4 (**8**)	$C_{93}H_{143}FN_{20}O_{18}S$	1879.1	941.7 $[M+2H]^{2+}$	3.0	+131	31

*via ESI-MS; **Retention time in minutes; ‡recorded in MeOH; §Overall % yield

 doi:10.20944/preprints202411.0510.v1

3.1. Circular Dichroism (CD) and Secondary Structure Analysis

The circular dichroism (CD) spectra of temporin NST-2 (**1**) and its analogs in 20 mM SDS are displayed in the Figure 1. Spectra show that in lipid-like environments provided by SDS, all analogs adopt an alpha-helical conformation due to their amphipathic properties, which is crucial for their antimicrobial function by facilitating their insertion into bacterial membranes. The hydrophobic segment of the peptide interacts with the lipid's hydrophobic portion, while the hydrophilic segment remains accessible to the aqueous environment. The percentage of alpha-helix and other secondary structures were quantified from CD data using Bestsel software (https://bestsel.elte.hu/index.php) and are shown in Table 3. NST-2 (**1**) exhibited an 81.5% alpha-helical content, while its retro analog RNST (**2**) displayed a 62% alpha-helical structure, showing that inversing amino acid sequence had major effect on secondary structure of NST-2. Addition of Lys at the C-terminus in analog **3** restaured the percentage of alpha-helix to 81.8 % whereas Lys substitution at position 4 in analog **7** decreased further helix content to 56.8 %. Conjugation with levofloxacin on Lys^{3} (analog **4**) or Lys^{14} (analog **5**) also restaured the helix content to 80.1 and 80.4 %, respectively. Conjugation with levofloxacin on Phe^{1} (analogs **6** and **8**) also increased alpha-helical content compared to analog **2** with 82.2 and 75.0%, respectively.

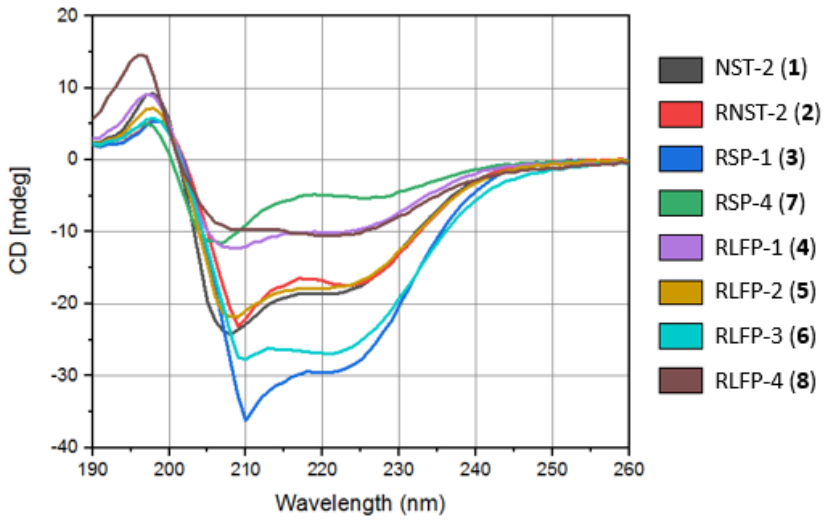

Figure 1. Circular dichroism of temporin NST-2, and newly synthesised analogs in 20 mM SDS.

Table 3. Percentage of the different types of secondary structures determined from CD data using Bestsel (https://bestsel.elte.hu/index.php).

Peptide	Helix (%)	Antiparallel (%)	Parallel (%)	Turn (%)	Others (%)
NST-2 (**1**)	81.5	18.5	0.00	0.00	0.00
RNST (**2**)	62.0	17.9	20.1	0.00	0.00
RSP-1 (**3**)	81.8	18.2	0.00	0.00	0.00
RLFP-1 (**4**)	80.1	19.9	0.00	0.00	0.00
RLFP-2 (**5**)	80.4	19.6	0.00	0.00	0.00
RLFP-3 (**6**)	82.2	17.8	0.00	0.00	0.00
RSP-4 (**7**)	56.8	22.1	0.00	7.6	13.6
RLFP-4 (**8**)	75.0	0.00	14.1	0.00	11.0

3.2. Antimicrobial Assay

NST-2 (**1**) has been already reported to possess strong antibacterial activity against Helicobacter pylori (ATCC 43504) and Staphylococcus aureus (NCTC 13277) with low hemolytic effect [28,29]. The

 doi:10.20944/preprints202411.0510.v1

retro analog of **1**, RNST-2 (**2**), was remarkably active against S. aureus (NCTC 13277), B. subtilis (ATCC 23857), S. typhi (ATCC 14028), E. coli (ATCC 25922), and P. aeruginosa (ATCC 10145) as well as against Candida albicans (ATCC 36082) (Table 4) with MIC values lower than the ones of **1** in all cases. Similarly, RSP-1 peptide (**3**) obtained by addition of Lys at the C-terminal end of analog **2** also showed higher antimicrobial activities compared to **1**. Further modifications were explored by synthesizing RSP-4 (**7**), an analog of **2** wherein Gly^4 was substituted with Lys. Although supposed to increase it, this substitution did not improve the antibacterial activity of the analog and rather inhibited it as evident from higher MIC values compared to **2**. The antibacterial molecule levofloxacin was then conjugated to some analogs to try to improve their activity. As expected, the addition of levofloxacin at position 1 in analog **7** via β-alanine linker generated RLFP-4 (**8**) with an improved activity against both Gram-positive and -negative bacteria but not against C. albicans. Similarly, RLFP-3 (**6**), wherein levofloxacin was again conjugated to Phe^1 of analog **3** also via β-alanine linker, demonstrated potent activities against both Gram-positive and -negative bacteria. Surprisingly and not expected due to the selective antibacteria activity of levofloxacin, it was also the most active analog against C. albicans with an MIC of 3.12 μM. In contrast to analogs **6** and **8**, RLFP-1 (**4**) and RLFP-2 (**5**) obtained by conjugation with levofloxacin to the side chain of Lys^{14} or Lys^3 of analog **3** displayed reduced antimicrobial effect compared to parent analog **3**.

Table 4. MIC value (in μM) of peptide analogues against different strains of bacteria and fungi.

Peptide	*S. aureus* (NCTC 13277)	*B. subtilis* (ATCC 23857)	*S. typhi* (ATCC 14028)	*E. coli* (ATCC 25922)	*P. aeruginosa* (ATCC 10145)	*C. albicans* (ATCC 36082)
NST-2 (**1**)	14.34	6.25	250	125	>250	20
RNST-2 (**2**)	3.12	1.56	50	50	200	15.6
RSP-1 (**3**)	6.25	1.56	50	25	50	15.6
RLFP-1 (**4**)	50	50	25	>200	>200	>250
RLFP-2 (**5**)	100	50	200	>200	>200	>250
RLFP-3 (**6**)	12.5	1.56	3.12	25	12.5	3.12
RSP-4 (**7**)	50	12.5	100	50	200	100
RLFP-4 (**8**)	6.25	1.56	50	25	12.5	>200

To further explore the mechanism of action of the analogs, three bacterial strains (S. typhi, E. coli, and P. aeruginosa) were treated with the most potent peptide analogs and analyzed through AFM technique in tapping mode. Figures-2 (A–D), 3 (A–D), and 4 (A–D) represents the S. typhi, E. coli, and P. aeruginosa bacteria, respectively. Untreated S. typhi (Figure 2A) appeared as short rods ranging its length between 0.8–1.5 μm, slightly irregular texture with no signs of damage or disruption. S. typhi treated with RLFP-4 (**8**), RLFP-3 (**6**), and RLFP-1 (**4**) at 2XMIC showed loss of morphological rod shapes. Loss of structural integrity could be seen due to leakage of cytoplasmic contents around the damaged cells demonstrating that the analogs caused membrane damages. Similarly, treatment of E. coli (Figure 3) or P. aeruginosa (Figure 4) with RLFP-3 (**6**), RSP-1 (**3**), and RLFP-4 (**8**) at 2XMIC values caused significant damages to the bacteria as their rod shaped morphology were lost, cells were disintegrated, and their cytoplasmic content were found around some rod shaped cells confirming again the membrane damages caused by the analogs.

 doi:10.20944/preprints202411.0510.v1

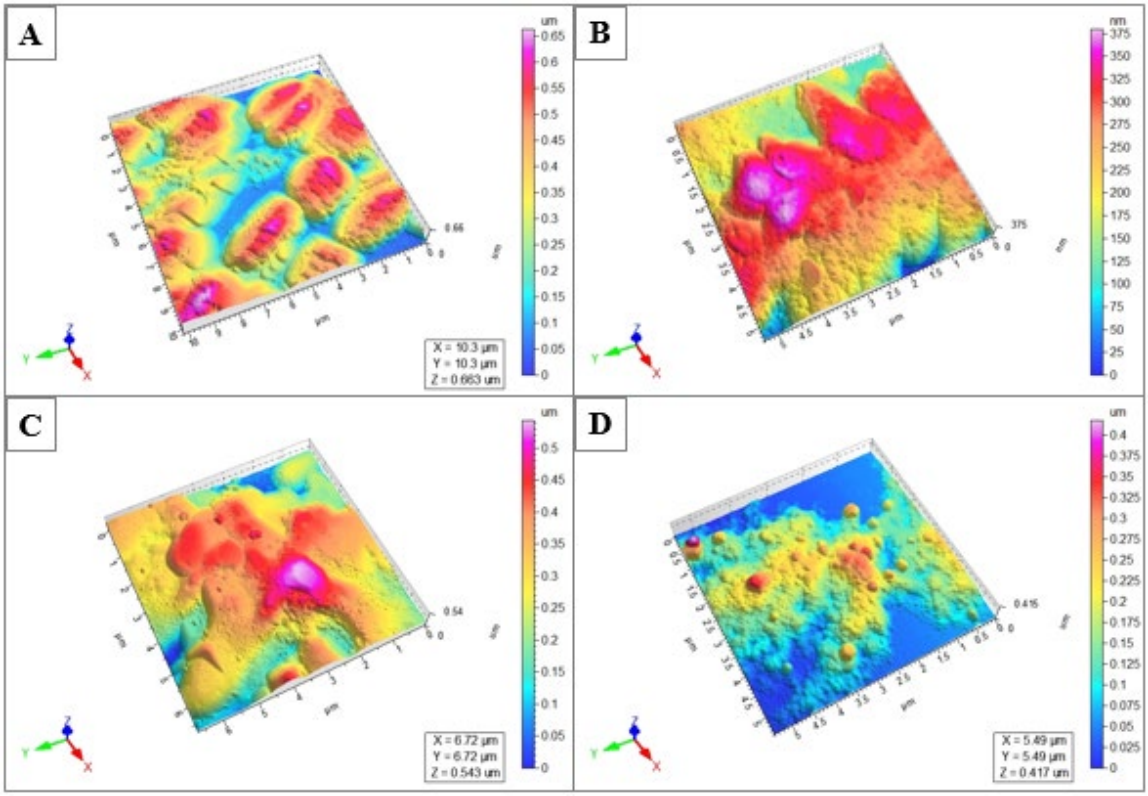

Figure 2. Atomic force microscopy images of Salmonella typhi after treatment; A) Untreated S. typhi; B) S. typhi treated with 100 µM of RLFP-4 peptide (**8**); C) S. typhi treated with 6 µM of RLFP-3 peptide (**6**); D) S. typhi treated with 50 µM of RLFP-1 peptide (**4**).

 doi:10.20944/preprints202411.0510.v1

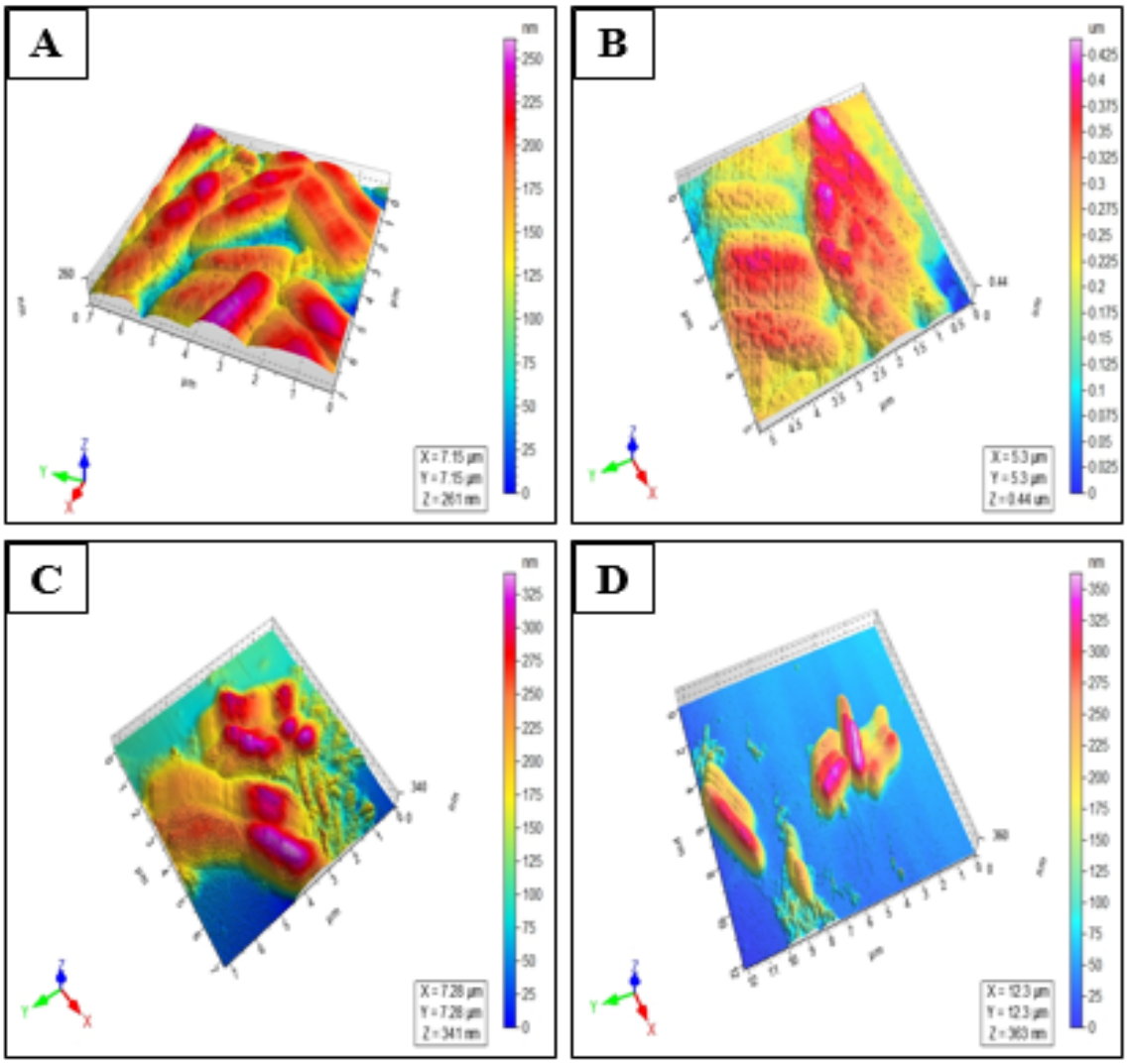

Figure 3. Atomic force microscopy of Escherichia coli after treatment; A) Untreated E. coli; B) After 50 μM treatment with RLFP-4 peptide (**8**); C) After 100 μM treatment with RSP-4 peptide (**7**); D) After 50 μM treatment with RLFP-3 peptide (**6**).

 doi:10.20944/preprints202411.0510.v1

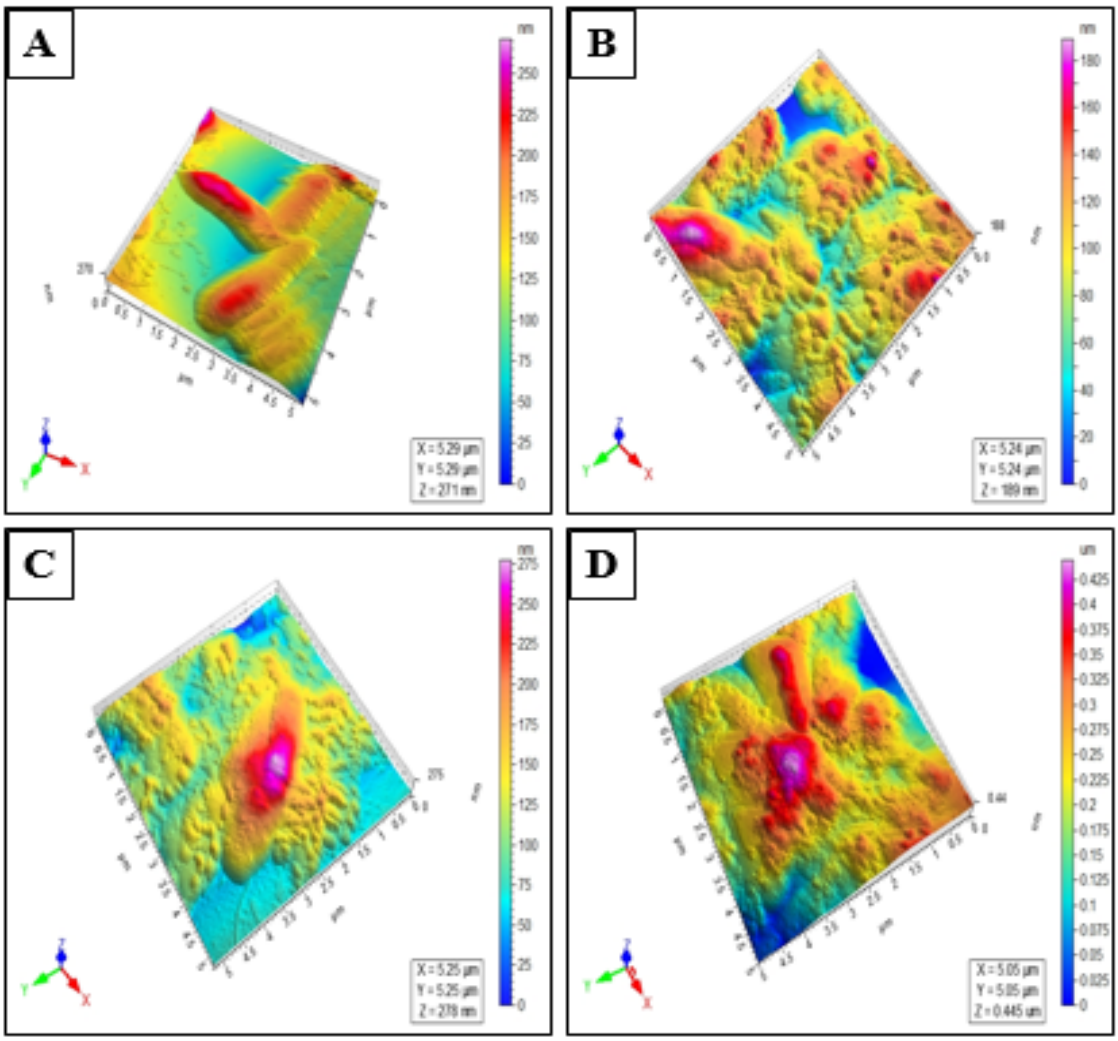

Figure 4. Atomic force microscopy of Pseudomonas aeruginosa after treatment; A) Untreated control; B) After 25 μM treatment with RLFP-3 peptide (**6**); C) After treatment with 100 μM of RSP-1 peptide (**3**); D) After treatment with 25 μM of RLFP-4 peptide (**8**).

3.3. Anticancer Activity and Hemolytic Effect of the Analogs

NST-2 (**1**) was previously reported with antibreast cancer activity (IC_{50}: 17.5 μM) in MCF-7 cells, while it was inactive against cervical cancer HeLa cells [32] with hemolysis HC_{50} value of 90.0 μM [29]. The antiproliferative activity of the retro analog of NST-2 against cancer cells, i.e., MCF-7 and HeLa cells, as well as their hemolytic properties are presented in Figure 5. IC_{50} and HC_{50} values were determined from Figure 5 and are reported in Table 5. Compared to parent peptide NST-2 (**1**), retro analog **2** was found less active on MCF-7 (Figure 5A) (IC_{50} of 17.9 versus 53.0 μM) but more active on HeLa (Figure 5B) (IC_{50} of > 100 versus 60.0 μM). Compared to parent analog **2**, analogs **3**, **6**, **7**, and **8** in which Lys was added were found more active than **2** on MCF-7 cells with an efficiency order of **6** > **8** > **7** > **3** > **2**. On HeLa cells, analogs **3**, **7**, and **8** were found more active than analog **2** with efficiency order of **8** > **3** > **7** > **2**. Analogs **4** and **5** in which levofloxacin was added to side chain of Lys^{14} or Lys^{3} were found inactive with IC_{50} > 100μM. Interestingly, analog **6** was the only analog with an IC_{50} on MCF-7 cells lower than the one of parent peptide NST-2 (**1**) (i.e., 13.3 versus 17.9 μM, respectively). But like analog **1**, analog **6** was found inactive on HeLa cells (IC_{50} > 100 μM).

Preprints.org (www.preprints.org) | NOT PEER-REVIEWED | Posted: 7 November 2024 doi:10.20944/preprints202411.0510.v1

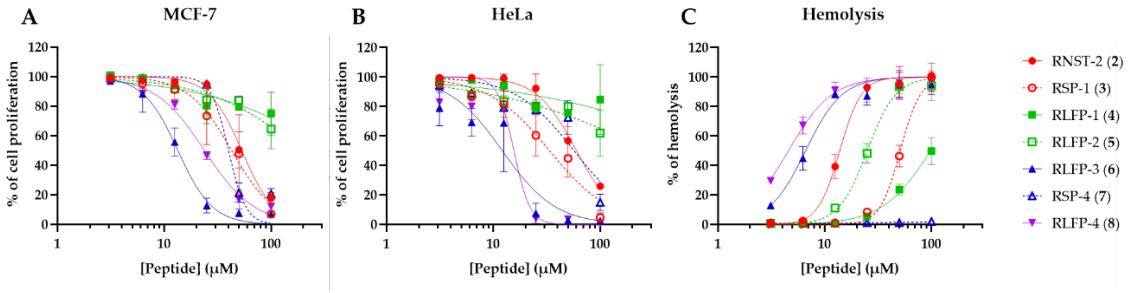

Figure 5. Dose-dependent antiproliferative and hemolytic effect of analogs. Antiproliferative effect of the analogs was measured after exposure of MCF-7 (**A**) or HeLa cells (**B**) to increasing concentrations of analogs for 24 hours.. Hemolytic effect of the analogs was measured after exposure of human red blood cells to increasing concentrations of analogs for 1 hour. Data were plotted using GrapPad Prism 8 (means +/- SD, n=3).

Table 5. Antiproliferative activity and hemolytic effect of analogs in term of inhibitory concentration 50% (IC_{50}), and hemolytic concentration 50% (HC_{50}) (in µM determined from Figure 5 using GraphPad Prism 8).

Peptide	Breast Cancer (MCF-7)	Cervical Cancer (HeLa)	Hemolysis (HC_{50})
NST-2 (**1**)	17.9	>100	90.0
RNST-2 (**2**)	53.0	60.0	13.8
RSP-1 (**3**)	42.7	33.5	51.0
RLFP-1 (**4**)	>100	>100	98.9
RLFP-2 (**5**)	>100	>100	25.0
RLFP-3 (**6**)	13.3	>100	6.6
RSP-4 (**7**)	39.9	56.9	>100
RLFP-4 (**8**)	23.8	15.5	4.5

In term of hemolysis (Figure 5C and Table 5), all analogs were found more hemolytic than analog **1** (with HC_{50} values ranging from 4.5 to 51.0 µM compared to 90.0 µM), except analog **4** with a similar HC_{50} (i.e., 98.9 µM) and analog **7** that was found not hemolytic at the tested concentrations (HC_{50} > 100 µM). When comparing with their parent molecule (i.e., the analog **2**), analogs **3**, **4**, **5**, and **7** were found less hemolytic than analog **2** (HC_{50} values of 51.0, 98.9, 25.0, and >100 µM versus 13.8 µM) confirming that the addition of Lys to AMPs sequences reduces their hemolytic effect. Oppositely, analogs **6** and **8** in which levofloxacin was added at position 1 were found more hemolytic than **2** (HC_{50} of 6.6 and 4.5 µM versus 13.8 µM, respectively).

3.4. Selectivity Indexes of the Analogs

The selectivity of action of the analogs against micro-organisms or cancer cells was further evaluated through calculation of their Selectivity Indexes (SI). SI were determined using either MIC on micro-organisms or IC_{50} on cancer cells compared to HC_{50} values, and are reported in Table 6.

Table 6. Selectivity indexes (SI) of analogs. SI were calculated by diving HC_{50} value (in µM, from Table 5) of each analog by its lowest MIC value on micro-organisms (in µM, from Table 4) or its lowest IC_{50} value on cancer cells (in µM, from Table 5).

Peptide	Lower MIC	Lower IC_{50}	Hemolysis (HC_{50})	SI based on MIC	SI based on IC_{50}
NST-2 (**1**)	6.25	17.9	90.0	14.4	5.0
RNST-2 (**2**)	1.56	53.0	13.8	8.8	0.2
RSP-1 (**3**)	1.56	33.5	51.0	32.6	1.5
RLFP-1 (**4**)	25	>100	98.9	3.9	<0.9

 doi:10.20944/preprints202411.0510.v1

RLFP-2 (**5**)	50	>100	25.0	0.5	<0.2
RLFP-3 (**6**)	1.56	13.3	6.6	4.2	0.4
RSP-4 (**7**)	12.5	39.9	>100	>8.0	>2.5
RLFP-4 (**8**)	1.56	15.5	4.5	2.8	0.2

Regarding SI on micro-organisms, it appears that the retro analog **2** has a lower SI compared to analog **1** (i.e., 8.8 versus 14.4). When comparing to parent analog **2**, all other analogs derived from **2** were also found less selective (due to higher MIC values and/or lower HC_{50}), except analogs **3** and **7**, for which SI on micro-organisms were equal (for **7**) or superior (3.7-fold increase for **3**) to parent analog **2**. This confirmed that addition of Lys into AMPs improves their selectivity through increased antimicrobial activity and/or decreased toxicity toward human cells, this being the case for analog **3** with an decreased toxicity (HC_{50} of 13.8 versus 51.0 µM for analogs **2** and **3**) with a conserved antimicrobial activity (lowest MIC of 1.56 µM for analogs **2** and **3**). Regarding levofloxacin conjugate analogs, their selectivity was reduced either due to decrease in antimicrobial effect or to increase in their toxicity. Analog **4** corresponding to levofloxacin conjugate on Lys^{14} displayed reduced toxicity (HC_{50} of 98.6 µM versus 13.8 µM for analog **2**) but also unfortunately reduced antimicrobial activity (lowest MIC of 25 µM for **4** versus 1.56 µM for **2**) resulting in a SI of 3.9 versus 8.8. Analogs **6** and **8** corresponding to levofloxacin conjugates at position 1 were as active as analog **2** (lowest MIC of 1.56 µM) but their higher toxicity (HC_{50} of 6.6 and 4.5 µM versus 13.8 µM) reduced their selectivity from 8.8 to 4.2 and 2.8, respectively. Regarding SI on cancer cells, all analogs were less selective than analog **1**, but when compared to analog **2** from which they originated, analogs **3**, **6**, and **7** were found more selective, suggesting again that the presence of additional Lys in the sequence of retro NST-2 improves its selectivity also against cancer cells.

4. Discussion

In the present study, retro analogs of NST-2, a D-alanine variant of temporin-SHa were synthetized and tested in term of antimicrobial and anticancer activities. This strategy was based on the fact that retro analogs of peptides have been described in the literature as more active than their parent peptides [8–11]. Retro analogs were further modified by addition of lysine residue, a strategy also known to improve AMPs activity and to decrease their hemolytic effect [35–37]. Finally, retro analogs were conjugated to levofloxacin (either on side chain of Lys or at the N-terminus of the peptide), the literature describing AMPs conjugated to antibiotics displaying or not increased efficiency depending of their sequences and site of conjugation [12–24]. Analogs were tested in term of antimicrobial, anticancer, and hemolytic activities.

In term of antimicrobial activity, previous works have shown that NST-2 (**1**) possesses strong antibacterial activity with low hemolytic effect [28,29]. The retro analog of **1**, RNST-2 (**2**), was remarkably active against both Gram-positive and Gram–negative bacteria as well as against Candida albicans with MIC values lower than the ones of **1** in all cases. This result confirmed that retro analogs possesse stronger antimicrobial activity compared to parent AMPs as described in the literature [8–10]. Similarly, RSP-1 peptide (**3**) obtained by addition of Lys at the C-terminal end of analog **2** also showed higher antimicrobial activities compared to NST-2 (**1**) but similar activity compared to retro NST-2 (**2**) except for E. coli and P. aeruginosa with an improved activity. This is in line with the literature showing that Lys addition to AMPs improves their antimicrobial activity [35–37]. Interestingly, RSP-4 (**7**), an analog of **2** wherein Gly^4 was substituted with Lys was found less active than NST-2 (**1**) or retro NST-2 (**2**) demonstrating that the site of Lys addition/substitution is critical in enhancing the activity of AMPs. Similarly, the site/type of conjugation of AMPs with levofloxacin influences the activity of the analogs. Conjugation with levofloxacin at the N-terminus of Phe^1 through β-alanine linker in analogs **6** and **8** improved activity against both Gram-positive and Gram-negative bacteria as described in the literature for some AMPs conjugated to levofloxacin. Surprisingly, and not expected due to the selective antibacterial activity of levofloxacin, conjugation to levofloxacin on Phe^1 also improved the antifungal activity of analog **6** but not analog **8** against C. albicans. Importantly, analog **6** was also the most active analog against C. albicans with an MIC of

 doi:10.20944/preprints202411.0510.v1

3.12 µM compared to 20.0 and 15.6 µM for NST-2 (**1**) and retro NST-2 (**2**), respectively. In contrast to analogs **6** and **8**, RLFP-1 (**4**) and RLFP-2 (**5**) obtained by the conjugation of levofloxacin to the side chain of Lys^{14} or Lys^{3} displayed reduced antimicrobial effect compared to parent analog **3** reinforcing the idea that modifications have different effect depending of the site/amino-acid modified.

Regarding anticancer activity, retro NST-2 (**2**) was found less active than parent NST-2 (**1**) on MCF-7 but more active on HeLa cells. In accordance with the literature, the addition of Lys at the C-terminus in analog **3** and the substitution of Gly to Lys at position 4 in analog **7** both increased the anticancer activity against MCF-7 and HeLa cells. Surprinsingly and not expected due to the selective antibacterial action of levofloxacin, the conjugation with levofloxacin at Phe^{1} (analogs **6** and **8**) resulted in higher anticancer effect on MCF-7 cells whereas on HeLa cells, only analog **8** showed increased activity. Analogs **4** and **5** in which levofloxacin was conjugated to side chain of Lys^{14} or Lys^{3} were found inactive with IC_{50} > 100µM showing that the site of conjugation to levofloxacin influences the anticancer activity of the analogs as observed for antimicrobial activity.

In term of hemolytic effect, retro NST-2 (**2**) unfortunately was found more hemolytic than the parent NST-2 (**1**) (HC_{50} of 13.8 versus 90.0 µM). Regarding other analogs, when comparing with their parent molecule (i.e., the analog **2**), analogs **3**, **4**, **5**, and **7**, all containing additional Lys, were found less hemolytic than analog **2** (HC_{50} values of 51.0, 98.9, 25.0, and >100 µM versus 13.8 µM) confirming that the addition of Lys to AMPs sequences reduces their hemolytic effect. Oppositely and surprisingly as levofloxacin by it-self is not hemolytic, analogs **6** and **8** in which levofloxacin was added on Phe^{1} were found more hemolytic than **2** (HC_{50} of 6.6 and 4.5 µM versus 13.8 µM, respectively).

Although a high percentage of alpha helix seems to be important for the antimicrobial activity of different AMPs, our data did not found such dependency for NST-2 retro analogs. Indeed, analogs with the higher percentage of helix were not necessary the ones giving the lowest MIC. Although analogs **3** and **6** with 81.8 and 82.2 % helix gave good activity (MIC as low as 1.56 µM), analogs **4** and **5**, with 80.1 and 80.4 % helix are the less active analogs (MIC ranging from 25 to >200 µM). Oppositely, analogs **2** and **8** with 62 and 75 % helix were found very active (MIC as low as 1.56 µM). The percentage of alpha-helix in analogs does not seems to correlate also with their anticancer activity. Indeed, the efficiency order in term of anticancer activity on MCF-7 was found as **6** (82.2% helix) > **8** (75.0% helix) > **7** (56.8% helix) > **3** (81.8% helix) > **2** (62.0% helix) with **4** (80.1% helix) and **5** (80.4% helix) being inactive. Similarly, no correlation was found between the percentage of alpha-helix and hemolytic activity of the analogs, since analogs with high percentage of alpha-helix e.g., analogs **1**, **4**, and **6** (81.5, 80.1, and 82.2% helix) have HC_{50} of 90.0, 98.9, and 6.6 µM, respectively.

As the modifications of the peptides affected both the activities and hemolytic effect of the analogs, the determination of their selectivity indexes (SI) was needed to identified best analog(s). Regarding antimicrobial activity, the selectivity indexes order was **3** > **1** > **2** = **7** > **6** > **4** > **8** > **5**. The retro analog of NST-2 (**2**) displays a lower SI compared to analog **1** (i.e., 8.8 versus 14.4) showing that although this analog is more active on micro-organisms, its parallel higher hemolytic effect reduces its selectivity. Addition of Lys in analogs **3** and **7** improves their SI by reducing their hemolytic effect compared to parent analog **2**, confirming that addition of Lys into AMPs improves their selectivity through decreased toxicity. Regarding levofloxacin conjugate analogs, their selectivity was reduced either due to decrease in antimicrobial effect (analogs **4** and **5**) or to increase in their hemolytic effect (analogs **6** and **8**). Regarding anticancer activity, the selectivity indexes order was **1** > **7** > **3** > **4** > **6** > **2** = **8** > **5**, all analogs being less selective than analog **1**, but when compared to analog **2** from which they originated, analogs **3**, **6**, and **7** were found more selective, suggesting again that the presence of additional Lys in the sequence of retro NST-2 analogs improves their selectivity also against cancer cells.

5. Conclusion

In this study, we explored the efficacy enhancement of an antimicrobial peptide, NST-2 (**1**), through retro analog synthesis, lysine addition / substitution, and levofloxacin conjugation. Although analog **2** corresponding to retro analog of NST-2 was found more active of bacteria and fungi, its

 doi:10.20944/preprints202411.0510.v1

higher hemolytic effect compared to parent NST-2 resulted in a reduction of its selectivity index and therapeutic potential. Addition of lysine (analog **3**) and lysine substitution (analog **7**) reduced the hemolytic effect of the analogs resulting in safer peptides. Conjugation with levofloxacin on lysine side chain (in analogs **4** and **5**) was found to decrease the hemolytic effect of the analogs but unfortunately also their antimicrobial and anticancer activities. Finally, conjugates obtained through addition of levofloxacin at the N-terminus of the peptide via β-alanine linker (analogs **6** and **8**) possessed increased antimicrobial and anticancer activity but also unfortunately increased hemolytic effect, resulting in less safe/selective analogs. In conclusion, lysine addition/substitution and levofloxacin conjugation to retro analog of NST-2, at least at the N-terminal position through β-alanine linker, were found to enhance their antimicrobial/anticancer activity and/or to decrease their hemolytic effect, enhancing their therapeutic potential.

Supplementary Materials: The following supporting information can be downloaded at the website of this paper posted on Preprints.org.

Funding: This work was supported by a grant 8169/Sindh/NRPU/R&D/HEC/2017 from the Higher Education Commission, Pakistan. Authors acknowledge the financial support from Higher Education Commission, Pakistan.

Author Contributions: Conceptualisation, F.S. and M.M; methodology, F.S. and M.M.; validation, F.S., M.M., F.-A.K. and S.N.; formal analysis, A.I.K., S.N., R.M., F.-A.K., M.M., F.S. and; investigation, A.I.K., M.M., F.S., S.N., S.N.K. and M.A.A.; writing—original draft preparation, S.N., F.-A.K., F.S., M.M., R.M., A.I.K., M.A.A. and S.N.K.; writing—review and editing, S.N., F.-A.K., M.M., F.S. and A.I.K.; supervision, F.-A.K., F.S. and M.M.; project administration, F.-A.K., F.S. and M.M.; funding acquisition, F.S. All authors have read and agreed to the published version of the manuscript.

Institutional Review: Not applicable.

Informed Consent Statement: Not applicable.

Data Availability Statement: All data are given in the main manuscript and SupplementaryMaterials.

Acknowledgments: Authors thank Dr. Yan Wang for verifying mass of the peptides. The authors also acknowledge the financial support from Higher Education Commission, Pakistan.

Conflicts of Interest: The authors declare no conflict of interest.

References

1. Xiao X, Lu H, Zhu W, Zhang Y, Huo X, Yang C, Xiao S, Zhang Y, Su J. A novel antimicrobial peptide derived from bony fish IFN1 exerts potent antimicrobial and anti-inflammatory activity in mammals. *Microbiology Spectrum* **2022**. 10(2): p. e02013-21.
2. Buommino E, Carotenuto A, Antignano I, Bellavita R, Casciaro B, Loffredo MR, Merlino F, Novellino E, Mangoni ML, Nocera FP, Brancaccio D, Punzi P, Roversi D, Ingenito R, Bianchi E, Grieco P. The Outcomes of Decorated Prolines in the Discovery of Antimicrobial Peptides from Temporin-L. **2019**. *ChemMedChem* 14(13): p. 1283-1290.
3. Bellavita R, Casciaro B, Di-Maro S, Brancaccio D, Carotenuto A, Falanga A, Cappiello F, Buommino E, Galdiero S, Novellino E, Grossmann TN, Mangoni ML, Merlino F, Grieco P. First-in-class cyclic Temporin L analogue: Design, synthesis, and antimicrobial assessment. *Journal of Medicinal Chemistry* **2021**. 64(15): p. 11675-11694.
4. Manteghi R, Pallagi E, Olajos G, Csoka I. Pegylation and formulation strategy of Anti-Microbial Peptide (AMP) according to the quality by design approach. *European Journal of Pharmaceutical Sciences* **2020**. 144: p. 105197.
5. Moreira Brito JC, Carvalho LR, De-Souza AN, Carneiro G, Magalhaes PP, Farias LM, Guimaraes NR, Verly RM, Resende Jm, De-Lima ME. PEGylation of the antimicrobial peptide LyeTx Ib maintains structure-related biological properties and improves selectivity. *Frontiers in Molecular Biosciences* **2022**. 9: p. 1001508.
6. Bednarska NG, Wren BW, Willcocks SJ. The importance of the glycosylation of antimicrobial peptides: Natural and synthetic approaches. *Drug Discovery Today* **2017**. 22(6): p. 919-926.
7. Jiang H, Zhang X, Chen X, Aramsantienchai P, Tong Z, Lin H. Protein lipidation: occurrence, mechanisms, biological functions, and enabling technologies. *Chemical Reviews* **2018**. 118(3): p. 919-988.
8. Rai J. Peptide and protein mimetics by retro and retroinverso analogs. *Chemical Biology and Drug Design* **2019**. 93(5): p. 724-736.

9. Nair DT, Kaur KJ, Singh K, Mukherjee P, Rajagopal D, George A, Bal V, Rath S, Rao KVS, Salunke DM. Mimicry of native peptide antigens by the corresponding retro-inverso analogs is dependent on their intrinsic structure and interaction propensities. *The Journal of Immunology* **2003**. 170(3): p. 1362-1373.
10. Chorev M. The partial retro–inverso modification: a road traveled together. *Peptide Science* **2005**. 80(2-3): p. 67-84.
11. Fletcher M.D. and Campbell M.M. Partially modified retro-inverso peptides: development, synthesis, and conformational behavior. *Chemical Reviews* **1998**. 98(2): p. 763-796.
12. Khan FA, Yaqoob S, Qasim MW, Ali S, Wang Y, Jiang ZH. A Robust, Gram-Scale and High-Yield Synthesis of MDP Congeners for Activation of the NOD2 Receptor and Vaccine Adjuvantation. *Synthesis* **2024**. 56(04): p. 539-548.
13. Guzelj S, Weiss M, Slutter B, Frkanec R, Jakopin Z. Covalently conjugated NOD2/TLR7 agonists are potent and versatile immune potentiators. *Journal of Medicinal Chemistry* **2022**. 65(22): p. 15085-15101.
14. Khan FA, Khanam R, Wasim Qasim M, Wang Y, Jiang ZH. Improved Synthesis of D-Isoglutamine: Rapid Access to Desmuramyl Analogues of Muramyl Dipeptide for the Activation of Intracellular NOD2 Receptor and Vaccine Adjuvant Applications. *European Journal of Organic Chemistry* **2021.** (48): p. 6688-6699.
15. Aamra H, Khan FA, Jahan H, Zafar M, Ali H, Shaheen F. Synthesis of novel benzimidazole containing antimicrobial peptides (AMPs) with significant inhibitory effect on multidrug resistant strain of *Salmonella typhimurium*. *Synthetic Communications* **2021**. 51(23): p. 3620-3628.
16. Gattu R, Ramesh SS, Nadigar S, Ramesh S. Conjugation as a tool in therapeutics: Role of amino acids/peptides-bioactive (including Heterocycles) hybrid molecules in treating infectious diseases. *Antibiotics* **2023**. 12(3): p. 532.
17. Khan FA, Nasim N, Wang Y, Alhazmi A, Sanam M, Ul-Haq Z, Yalamti D, Ulanova M, Jiang ZH. Amphiphilic desmuramyl peptides for the rational design of new vaccine adjuvants: synthesis, in vitro modulation of inflammatory response and molecular docking studies. *European Journal of Medicinal Chemistry* **2021**. 209: p. 112863.
18. Khan FA, Ulanova M, Bai B, Yalamati D, Jiang ZH. Design, synthesis and immunological evaluation of novel amphiphilic desmuramyl peptides. *European Journal of Medicinal Chemistry* **2017**. 141: p. 26-36.
19. Gobec M, Tomašič T, Štimac A, Frkanec R, Trontelj J, Anderluh M, Mlinaric-Rascn I, Jakopin Z. Discovery of nanomolar desmuramylpeptide agonists of the innate immune receptor nucleotide-binding oligomerization domain-containing protein 2 (NOD2) possessing immunostimulatory properties. *Journal of Medicinal Chemistry* **2018**. 61(7): p. 2707-2724.
20. Guzelj S, Nabergoj S, Gobec M, Pajk S, Klančič V, Slütter B, Frkanec R, Stimac A, Sket P, Plavec J, Mlinaric-Rascan I, Jakopin Z. Structural fine-tuning of desmuramylpeptide NOD2 agonists defines their in vivo adjuvant activity. *Journal of Medicinal Chemistry* **2021**. 64(11): p. 7809-7838.
21. Reinhardt A, Neundorf I. Design and application of antimicrobial peptide conjugates. *International Journal of Molecular Sciences* **2016**. 17(5): p. 701.
22. 22 Ceccherini F, Falciani C, Onori M, Scali S, Rossolini GM, Bracci L, Pini A. Antimicrobial activity of levofloxacin–M33 peptide conjugation or combination. *MedChemComm* **2016**. 7(2): p. 258-262.
23. Riahifard N, Tavakoli K, Yamaki J, Parang K, Tiwari R. Synthesis and evaluation of antimicrobial activity of [R4W4K]-Levofloxacin and [R4W4K]-Levofloxacin-Q conjugates. *Molecules* **2017**. 22(6): p. 957.
24. Sajid MI, Lohan S, Kato S, Tiwari RK. Combination of Amphiphilic Cyclic Peptide [R4W4] and Levofloxacin against Multidrug-Resistant Bacteria. *Antibiotics* **2022**. 11(3): p. 416.
25. Atzori A, Baker AE, Chiu M, Bryce RA, Bonnet P. Effect of sequence and stereochemistry reversal on p53 peptide mimicry. *PLoS One* **2013**. 8(7): p. e68723.
26. Zerze GH, Stillinger FH, Debenedetti PG. Computational investigation of retro-isomer equilibrium structures: Intrinsically disordered, foldable, and cyclic peptides. *FEBS Letters* **2020**. 594(1): p. 104-113.
27. Khan AI, Nazir S, Haque MNU, Maharjan R, Khan FA, Olleik H, Courvoisier-Dezord E, Maresca M, Shaheen F. Synthesis of Second-Generation Analogs of Temporin-SHa Peptide Having Broad-Spectrum Antibacterial and Anticancer Effects. *Antibiotics* **2024**. 13(8): p. 758.
28. Olleik H, Baydoun E, Perrier J, Hijazi A, Raymond J, Manzoni M, Dupuis L, Pauleau G, Goudard Y, de La Villéon B, Goin G, Sockeel P, Choudhary MI, Pasquale ED, Haque MNU, Ali H, Khan AI, Shaheen F, Maresca M. Temporin-SHa and its analogs as potential candidates for the treatment of *helicobacter pylori*. *Biomolecules* **2019**. 9(10): p. 598.
29. Maharjan R, Khan AI, Haque MNU, Maresca M, Choudhary MI, Shaheen F, Simjee SUA. Serum stable and low hemolytic temporin-SHa peptide analogs disrupt cell membrane of methicillin-resistant *Staphylococcus aureus* (MRSA). Probiotics *Antimicrob.* **2022**. 14(2): p. 391-405.
30. Khan, A.I.; Nazir, S.; Ullah, A.; Haque, M.N.u.; Maharjan, R.; Simjee, S.U.; Olleik, H.; Dezord, E.C.; Maresca, M.; Shaheen, F. Design, synthesis and characterization of [G10a]-Temporin SHa dendrimers as dual inhibitors of cancer and pathogenic microbes. *Biomolecules* **2022**. 12(6): p. 770.
31. Lucana MC, Arruga Y, Petrachi E, Roig A, Lucchi R, Oller-Salvia B. Protease-resistant peptides for targeting and intracellular delivery of Therapeutics. *Pharmaceutics* **2021**. 13(12): p. 2065.

 doi:10.20944/preprints202411.0510.v1

32. Shaheen F, Nadeem-ul-Haque M, Ahmed A, Simjee SU, Ganesan A, Jabeen A, Shah Z.A. Choudhary, M.I. Synthesis of breast cancer targeting conjugate of temporin-SHa analog and its effect on pro-and anti-apoptotic protein expression in MCF-7 cells. *Peptides* **2018**. 106: p. 68-82.
33. Lancaster M.V, Fields R.D. Antibiotic and cytotoxic drug susceptibility assays using resazurin and poising agents. *Biotechnology Advances*, **1997**. 15(1): p. 193-193.
34. Wiradharma N, Khoe U, Hauser CA, Seow SV, Zhang S, Yang YY. Synthetic cationic amphiphilic α-helical peptides as antimicrobial agents. *Biomaterials* **2011**. 32(8): p. 2204-2212.
35. Amirkhanov NV, Bardasheva AV, Tikunova NV, Pyshnyi DV. Synthetic antimicrobial peptides: III—Effect of cationic groups of lysine, arginine, and histidine on antimicrobial activity of peptides with a linear type of amphipathicity. *Russian Journal of Bioorganic Chemistry* **2021**. 47(3): p. 681-690.
36. Sato, H, Feix JB. Lysine-enriched cecropin-mellitin antimicrobial peptides with enhanced selectivity. *Antimicrobial Agents and Chemotherapy* **2008**. 52(12): p. 4463-4465.
37. Taheri B, Mohammadi M, Momenzadeh N, Farshadzadeh Z, Roozbehani M, Dehghani P. Substitution of lysine for isoleucine at the center of the nonpolar face of the antimicrobial peptide, piscidin-1, leads to an increase in the rapidity of bactericidal activity and a reduction in toxicity. *Infection and Drug Resistance* **2019**: p. 1629-1647.
38. Wang X, Zhang W, Wu W, Wu S, Young A, Yan Z. Candida albicans a contributor to cancer? A critical review based on the current evidence. *Microbiological Research* **2023**: p. 127370.
39. Raja Z, Andre S, Abbasi F, Humblot V, Lequin O, Bouceba T, Correia I, Casale S, Foulon T, Sereno D, Oury B, Ladram A. Insight into the mechanism of action of temporin-SHa, a new broad-spectrum antiparasitic and antibacterial agent. *PLoS One* **2017**. 12(3): p. e0174024.
40. D'Andrea L.D, Romanelli A. Temporins: multifunctional peptides from frog skin. *International Journal of Molecular Sciences* **2023**. 24(6): p. 5426.